View metadata, citation and similar papers at core.ac.uk
brought to you by CORE
provided by Helsingin yliopiston digitaalinen arkisto

REPORT SERIES IN AEROSOL SCIENCE
N:o 147 (2014)

EXPERIMENTAL STUDIES ON NUCLEATION AND ATMOSPHERIC AEROSOL PARTICLE FORMATION DOWN TO THE MOLECULAR LEVEL

SIEGFRIED SCHOBESBERGER

Division of Atmospheric Sciences
Department of Physics
Faculty of Science
University of Helsinki
Helsinki, Finland

Academic dissertation

To be presented, with the permission of the Faculty of Science of the University of Helsinki, for public criticism in auditorium E204, Gustaf Hällströminkatu 2a, on Friday, March 14th, 2014, at 12 o'clock noon.

Helsinki 2014

Author's Address: Division of Atmospheric Sciences
Department of Physics
P.O. Box 64
FI-00014 University of Helsinki
siegfried.schobesberger@helsinki.fi

Supervisors: Professor Markku Kulmala, Ph.D.
Department of Physics
University of Helsinki

Professor Tuukka Petäjä, Ph.D.
Department of Physics
University of Helsinki

Professor Douglas R. Worsnop, Ph.D.
Department of Physics
University of Helsinki

Reviewers: Professor Jyrki Mäkelä, Ph.D.
Tampere University of Technology

Docent Hannele Korhonen, Ph.D.
Finnish Meteorological Institute, Kuopio Unit

Opponent: Professor Hugh Coe, Ph.D.
School of Earth, Atmospheric and Environmental Sciences
University of Manchester, United Kingdom

ISBN 978-952-5822-84-7 (printed version)
ISSN 0784-3496
Helsinki 2014
Unigrafia Oy

ISBN 978-952-5822-85-4 (PDF version)
http://ethesis.helsinki.fi/
Helsinki 2014
Helsingin Yliopiston verkkojulkaisut

Acknowledgements

The research presented in this thesis was carried out at the Faculty of Physics of the University of Vienna and at the Department of Physics of the University of Helsinki. I want to thank the heads of these institutions for providing me the working facilities during my work on this thesis: Professors Anton Zeilinger, Juhani Keinonen and Hannu Koskinen.

I want to express my gratitude to Prof. Paul Wagner for introducing me into the elegant and satisfying way in which physics works in solving problems, and into the field of aerosol science and nucleation. I am very grateful to Prof. Markku Kulmala for having given me the opportunity of working in his division, for his support and efficient supervision, and for providing the tools and work environments that allowed me to pursue my PhD on the leading edge of atmospheric sciences.

I wish to thank Prof. Tuukka Petäjä for his guidance and collaboration during my PhD, for listening to my problems, and for the dispensed doses of you-can-do-it spirit. Big thanks go to Prof. Doug Worsnop for his support, guidance and advising, for his unshakable and motivating enthusiasm, and for the many great enjoyable and important discussions.

I thank Prof. Jyrki Mäkelä and Doc. Hannele Korhonen for reviewing this thesis.

Dr. Mikko Sipilä and Dr. Mikael Ehn are acknowledged for doing their parts in advising me, especially during the later parts of my PhD, for their collaboration and fruitful discussions. I also wish to thank Dr. Heikki Junninen for his helpful collaboration and support throughout, and for leading the development of the tofTools software package, without which much of this work would have been hard, some hardly possible. He has also served as my office mate longer than anyone else, and did so with distinction.

A problem shared is a problem halved: I want to express my big thanks to my colleague and friend Alessandro Franchin for sharing and halving so many problems and sorrows throughout my PhD. Our mutual support was as critical for our successes during campaigns, as it was for arriving sane at the end of my PhD studies.

I want to thank all my great colleagues that I have had the pleasure to work with, many of whom I call friends, for making this division such a nice environment to work in, as well as a world-class research group.

I feel grateful to all my co-authors who were indispensible and invaluable for getting all this work done. I am particularly grateful to the fellows who came to CERN to work day and night, often selflessly, to make the CLOUD experiments happen, and therefore much of this thesis.

Thanks to all my friends for giving me that comfortable and reassuring feeling of acceptance without asking for anything in return. Our times together have given me much-needed balance during these years. I want to express my gratitude to my parents, for their continuing unconditional support, and for providing a peaceful haven I can occasionally retreat to. And my deepest thanks go to Emmi Aro, for her companionship and love.

Experimental studies on nucleation and atmospheric aerosol particle formation down to the molecular level

Siegfried Schobesberger
University of Helsinki, 2014

Abstract

Aerosol particles in the atmosphere have effects on human health, as well as on the radiative forcing and therefore on climate. An important source of atmospheric aerosol is the formation of aerosol particles from gas-phase precursors. In this thesis, the main goal was to improve our understanding of the chemical and physical mechanisms via which this atmospheric particle formation proceeds.

Attempts have been made to describe aerosol particle formation by classical nucleation theory. To test this theory, the heterogeneous nucleation of n-propanol vapor on 4–11 nm NaCl and Ag seed particles was investigated. The choice of seed particle material was found to determine if classical theories could be applied or not. These observations were probably due to material-specific inter-molecular interactions between the vapor and the seed particle. The classical theories are based on macroscopic observations and fail to describe these interactions, which can be crucial in microscopic systems.

However, the critical processes of atmospheric particle formation occur at sizes below 2 nm. In this thesis, novel techniques were employed to access this size range, primarily the atmospheric pressure interface time-of-flight (APi-TOF) mass spectrometer. The APi-TOF directly measures the composition of ions and ionic clusters up to a size of about 2 nm. APi-TOFs were employed at the CLOUD facility at CERN during four comprehensive measurement campaigns, which focused on exploring particle formation from various systems of vapors. The APi-TOF measurements were extraordinarily successful. Its results were the key in revealing the detailed mechanisms of how clusters were initially formed by which vapors, and how these clusters grew to sizes > 2 nm. Clusters of sulfuric acid + ammonia and sulfuric acid + dimethylamine were shown to form and grow via strong hydrogen bonds between acidic and basic molecules. Cluster dynamics simulations, including quantum chemical calculations of cluster stabilities, agreed well with the experimental results. The APi-TOF measurements also showed that certain large monoterpene oxidation products, some of them very highly oxidized, can directly bind with bisulfate ions and with sulfuric acid molecules. The clusters then grow by the addition of more of these large oxidized organics and sulfuric acid molecules. Ion mass spectra from CLOUD experiments were compared with ion mass spectra from particle formation events in the boreal forest. Similarities suggest that large oxidized organics play a crucial role also in the ambient particle formation events.

A light airplane was used to explore how the mechanisms of actual aerosol particle formation vary throughout the atmosphere above the boreal forest. These airborne measurements reached from the canopy up into the lower free troposphere. They confirmed the extent of boundary layer new particle formation events, and showed indications of an important role of dynamical processes at the top of the boundary layer. Local enhancements of particle formation were observed in connection with clouds.

This thesis' goal was achieved chiefly by using state-of-the-art experimental techniques together with high-quality laboratory experiments as well as in the field, and by taking ambient measurements aloft. Hopes are that this work will prove to be an important contribution in advancing our knowledge of the physical and chemical mechanisms of atmospheric aerosol particle formation.

Keywords: Atmospheric aerosol, particle formation, ion clusters, nucleation, mass spectrometry, CLOUD experiment, airborne measurement

Contents

List of publications

This thesis consists of an introductory review, followed by five research articles. In the introductory part, these papers are cited according to their roman numerals.

I Schobesberger S., Winkler P. M., Pinterich T., Vrtala A., Kulmala M., Wagner P. E.: Experiments on the temperature dependence of heterogeneous nucleation on nanometer-sized NaCl and Ag particles, *ChemPhysChem*, 11, 3874–3882 (2010).

II Olenius T., Schobesberger S., Kupiainen O., Franchin A, Junninen H, Ortega IK, Kurtén T., Loukonen V., Worsnop D. R., Kulmala M., Vehkamäki H.: Comparing simulated and experimental molecular cluster distributions, *Farad. Discuss.*, 165, 75–89 (2013).

III Almeida J., Schobesberger S., Kürten A., Ortega I. K., Kupiainen-Määttä O., Praplan A. P., Adamov A., Amorim A., Bianchi F., Breitenlechner M., David A., Dommen J., Donahue N. M., Downard A., Dunne E., Duplissy J., Ehrhart S., Flagan R. C., Franchin A., Guida R., Hakala J., Hansel A., Heinritzi M., Henschel H., Jokinen T., Junninen H., Kajos M., Kangasluoma J., Keskinen H., Kupc A., Kurtén T., Kvashin A. N., Laaksonen A., Lehtipalo K., Leiminger M., Leppä J., Loukonen V., Makhmutov V., Mathot S., McGrath M. J., Nieminen T., Olenius T., Onnela A., Petäjä T., Riccobono F., Riipinen I., Rissanen M., Rondo L., Ruuskanen T., Santos F. D., Sarnela N., Schallhart S., Schnitzhofer R., Seinfeld J. H., Simon M., Sipilä M., Stozhkov Y., Stratmann F., Tomé A., Tröstl J., Tsagkogeorgas G., Vaattovaara P., Viisanen Y., Virtanen A., Vrtala A., Wagner P. E., Weingartner E., Wex H., Williamson C., Wimmer D., Ye P., Yli-Juuti T., Carslaw K. S., Kulmala M., Curtius J., Baltensperger U., Worsnop D. R., Vehkamäki H., Kirkby J.: Molecular understanding of sulphuric acid-amine particle nucleation in the atmosphere, *Nature*, 502, 359–363 (2013).

IV Schobesberger S., Junninen H., Bianchi F., Lönn G., Ehn M., Lehtipalo K., Dommen J., Ehrhart S., Ortega I. K., Franchin A., Nieminen T., Riccobono F., Hutterli M., Duplissy J., Almeida J., Amorim A., Breitenlechner M., Downard A. J., Dunne E. M., Flagan R. C., Kajos M., Keskinen H., Kirkby J., Kupc A., Kürten A., Kurtén T., Laaksonen A., Mathot S., Onnela A., Praplan A. P., Rondo L., Santos F. D., Schallhart S., Schnitzhofer R., Sipilä M., Tomé A., Tsagkogeorgas G., Vehkamäki H., Wimmer D., Baltensperger U., Carslaw K. S., Curtius J., Hansel A., Petäjä T., Kulmala M., Donahue N. M., Worsnop D. R.: Molecular understanding of atmospheric particle formation from sulfuric acid and large oxidized organic molecules, *Proc. Natl. Acad. Sci. USA*, 110, 17223–17228 (2013).

V Schobesberger S., Väänänen R., Leino K., Virkkula A., Backman J., Pohja T., Siivola E., Franchin A., Mikkilä J., Paramonov M., Aalto P. P., Krejci R., Petäjä T., Kulmala M.: Airborne measurements over the boreal forest of southern Finland during new particle formation events in 2009 and 2010, *Boreal Env. Res.*, 18, 145–163 (2013).

1 Introduction

1.1 Atmospheric aerosol

Aerosol is a suspension of liquid or solid particles in air or any other carrier gas. Aerosol particles are ubiquitous in the Earth's atmosphere. Typical particle number concentrations range from as low as about 20 cm^{-3} in the Antarctic winter (Järvinen et al., 2013), to about 20000 cm^{-3} in European cities (Gao et al., 2009), up to about 100000 cm^{-3} at highly polluted urban sites (Mönkkönen et al., 2005; Apte et al., 2011). Particle sizes range from 1 nm (10^{-9} m; the smallest molecular clusters) to 100 µm (10^{-4} m; large pollen, fly ash, coarse dust) (Hinds, 1999).

These atmospheric aerosol particles are of high interest for two reasons. Firstly, they generally have a negative impact on human health (Nel et al., 2006; Vaclavik Bräuner et al., 2007). Secondly, they have an impact on the climate by influencing the Earth's radiation balance by direct and indirect effects, both with a net cooling effect (Charlson et al., 1992; IPCC, 2007). The direct effect is the absorption and reflection of sunlight (Ångström, 1929), the indirect effect is the role that aerosol particles play in the formation of clouds (Scorer, 1967). Namely, aerosol particles larger than 50 to 100 nm in diameter can act as seeds, onto which water vapor can condense already at minimal supersaturations (i.e., at a relative humidity only slightly above 100%) to form cloud droplets (Fletcher, 1962; Andreae and Rosenfeld, 2008). The particles acting as seeds are termed cloud condensation nuclei (CCN). In a case of higher number concentrations of CCN, the condensing water is distributed to more seeds, leading to more numerous but smaller cloud droplets. Such droplets give the cloud both a higher reflectivity and a longer lifetime, resulting in a net cooling effect (Coakley et al., 1987).

Atmospheric aerosol particles have a variety of sources (Jaenicke, 1993). Aerosol can originate from the direct emission of particles. Direct sources are sea spray, fires, wind-blown dust, volcanoes, anthropogenic combustion processes, and emissions from the biosphere. Aerosol particles can also form in the atmosphere from vapors that form smallest particles (1 to 2 nm in size), which subsequently grow by the further condensation of vapors (Kulmala et al., 2004c). This process of new particle formation is usually referred to as nucleation.

1.2 Nucleation

From a macroscopic point-of-view, the co-condensation of vapor molecules to form liquid or solid particles involves a phase transition from the gas-phase to the liquid- or solid-phase. Therefore, this phenomenon is classically treated as a problem of thermodynamics. The classical approach assumes that the gas-phase behaves like an

ideal gas, and that the surface created by the condensed state is spherical and has a surface tension. A further simplifying assumption is that the surface tension is not affected by the curvature of the surface. In the simplest case, only one vapor and no foreign surfaces are involved (unary homogeneous nucleation). Under all these assumptions, it can be shown that the change of the system's Gibbs free energy for the formation of a liquid droplet *i* is

$$\Delta G_i = 4\pi\sigma {r_i}^2 - ik_BT \ln\frac{p_v}{p_s(T)} \quad [1]$$

r_i is the droplet's radius, σ is the surface tension, i is the number of vapor molecules in the liquid phase, k_B is the Boltzmann constant, T is the temperature, p_v is the partial vapor pressure, and $p_s(T)$ is the saturation vapor pressure, which is generally dependent on T (Fletcher, 1962). The ratio $p_v/p_s(T)$ is called the saturation ratio; ΔG_i is called the formation energy. For saturation ratios ≤ 1, the formation energy ΔG_i increases strictly monotonically as a function of r_i, i.e. no stable liquid clusters will form. For saturation ratios > 1, $\Delta G_i(r_i)$ has a maximum (ΔG^*) at a critical radius r^*. The relationship between r^* and the saturation ratio $p_v/p_s(T)$ is given by the Kelvin equation (Thomson, 1870, 1871). One form of the Kelvin equation is

$$\ln\frac{p_v}{p_s(T)} = \frac{2\sigma}{r^* n_l k_B T} \quad [2]$$

n_l is the number of molecules per volume in the condensed (liquid) phase. Eq. 2 generally describes the saturation ratio $p_v/p_s(T)$ of a vapor in equilibrium with a curved surface of the condensed phase, with r^* being the radius of curvature of that surface. r^* is called the critical radius, because at given conditions, a droplet with a smaller radius will evaporate, whereas a droplet surpassing the critical radius will grow (i.e., it nucleates). The nucleation rate J is the rate at which droplets reach a size just beyond r^*. J can be approximated by

$$J \cong K \exp\left(-\frac{\Delta G^*}{k_B T}\right) \quad [3]$$

using linear cluster kinetics and a Boltzmann distribution for the size distribution of droplets up to r^* (Abraham, 1969; Fletcher, 1962). K is a kinetic coefficient.

Nucleation can also occur on a pre-existing surface. The process is then known as heterogeneous nucleation, in particular if the pre-existing surface (= seed) is non-soluble. Eq. 2 is also valid for the heterogeneous nucleation on a non-soluble seed. However, in homogeneous nucleation a critical liquid droplet with radius r^* is formed, whereas in heterogeneous nucleation a critical liquid embryo is formed on the seed

surface. The embryo is in the shape of a spherical cap with a radius of curvature r^*. The seed surface assists in the formation of the critical embryo; correspondingly, the formation energy required to form the critical embryo, ΔG^*, is to be multiplied by a factor $0 \leq f \leq 1$ (Fletcher, 1958). f is a function of the contact angle of the liquid on the solid seed and of the ratio between the seed surface curvature and r^*. Multiplication by f generally reduces the nucleation barrier ΔG^*, therefore heterogeneous nucleation is preferred over homogeneous nucleation. In the atmosphere, homogeneous nucleation of water does not occur at all, because seed surfaces are readily available, in particular in the form of pre-existing aerosol particles.

Note that the nucleation of droplets on spherical aerosol seed particles is expected to occur on seed particles with a radius smaller than r^*, in particular for seed particles < 10 nm in diameter (Fletcher, 1958). Experimentally, it was shown that this consequence of classical heterogeneous nucleation theory holds quantitatively even down to seed particle sizes of only 2 nm in mobility-equivalent diameter, at least for certain combinations of vapor and seed (Winkler et al., 2008a).

An additional way of reducing the height of the nucleation barrier ΔG^* is the nucleation on an electrically charged seed or on a molecular ion (ion-induced nucleation), as the electrostatic interactions between the charged core and ligand molecules reduce ΔG^* (Curtius et al., 2007). Terms that describe these interactions are added to Eq. 1 and to Eq. 2 for the ion-induced case. The thus extended form of Eq. 2 is known as the Kelvin-Thomson equation (Thomson, 1906; Girshick and Chiu, 1990; Winkler et al., 2012).

Yet another way of reducing the formation energy of clusters is the co-condensation of more than one vapor to form a solution droplet or embryo (multi-component nucleation; Vehkamäki, 2006). In Eq. 1, values of the solution liquid have to be used for σ and $p_s(T)$, and the equation is modified by adding a term $-i_x k_B T \ln \frac{p_{v,x}}{p_s(T)}$ for each additional condensing vapor x (Kulmala and Viisanen, 1991). $p_{v,x}$ is the partial vapor pressure of x, and i_x the number of molecules of x in the liquid phase. The formation energy for a liquid cluster, ΔG, is now a function of all i_x. The function usually forms a saddle point at a certain set of values for each i_x. This saddle point corresponds to the critical liquid cluster. The critical cluster's formation energy, ΔG^*, is then smaller than for the case of the unary nucleation of any one vapor x (e.g. Yue and Hamill, 1979; Strey et al., 1995).

A related nucleation process of atmospheric importance is the heterogeneous nucleation of water on a soluble seed particle. This process is described by Köhler theory. It uses Raoult's law to obtain the vapor pressures of the solution and its components (Raoult, 1887, 1888). The Kelvin equation (Eq. 2) is correspondingly modified to obtain the equilibrium vapor pressure of water over the solution droplet as a function of droplet size (Köhler, 1936). Köhler theory and modifications thereof describe the formation of haze, mist and cloud droplets on hygroscopic aerosol particles (e.g., Laaksonen et al.,

1998). The latter is commonly referred to as CCN activation. Turbulent fluctuations can facilitate the formation and growth of cloud droplets also at mean saturation ratios below one (Kulmala et al., 1997).

1.3 Mechanisms of atmospheric new particle formation

New particle formation in the atmosphere from condensable vapors is believed to be a major source of climatically relevant aerosol. It may account for up to 50% of global CCN (Merikanto et al., 2009). Newly formed particles are subject to loss mechanisms that may prevent them from growing big enough to act as CCN, mainly due to the loss by coagulation with pre-existing particles (Kulmala et al., 2001a; Dal Maso et al., 2002; Vehkamäki and Riipinen, 2012). Therefore, it is important to understand both the formation of particles from vapor precursors and the subsequent growth of these particles to 50–100 nm in diameter, at which they can act as CCN.

In particular the very first steps of this process have long been poorly understood. One compound that is very likely involved in atmospheric new particle formation is sulfuric acid (Weber et al., 1996; Riipinen et al., 2007; Sipilä et al., 2010). Binary homogeneous nucleation of water and sulfuric acid (H_2SO_4) is probably able to account for particles in the relatively cold upper troposphere (Lovejoy et al., 2004). But H_2SO_4 concentrations ($[H_2SO_4]$) are too low to explain new particle formation by binary homogeneous nucleation in the lower troposphere's boundary layer (Kirkby et al., 2011).

Kulmala et al. (2004a) derived a mechanism known as Nano-Köhler theory from classical thermodynamics to explain boundary layer particle formation. This mechanism consists of a two-step process: multi-component homogeneous nucleation of water (H_2O), ammonia (NH_3), and H_2SO_4 to form small (1–3 nm) thermodynamically stable clusters, followed by the activation of these clusters by organic vapors in an analogue way to Köhler theory. Recently, experimental evidence was found for such a two-step process being the initial mechanism of atmospheric particle formation, although the exact details remained vague (Kulmala et al., 2013).

It may be questioned if mechanisms derived from macroscopic physics are able to explain the critical processes in the very first steps of particle formation, because they occur well below a size of 2 nm of mobility-equivalent diameter (Kulmala et al., 2013). Therefore, they involve clusters of only a few molecules. Specific interactions between single molecules or chemical reactions may play dominant roles that cannot be deduced from macroscopic observations.

Most likely, the first steps of boundary layer particle formation involve the stabilization of only few H_2SO_4 molecules (Petäjä et al., 2011). Interactions with ubiquitous H_2O molecules are probably involved. It has been shown that H_2SO_4 molecules can be much

more strongly stabilized by forming clusters with ions (Lovejoy et al., 2004), with bases such as ammonia (Ortega et al., 2008) and amines (Kurtén et al., 2008), or with oxygenated organic molecules (Zhao et al., 2009; Metzger et al., 2010; Zhang et al., 2004). The initially resulting molecular clusters are small (< 3 nm in size) and therefore prone to be lost by coagulation (Dal Maso et al., 2002). Consequently, the clusters have to be stable enough and the availability of the participating vapors high enough to allow for the growth of the clusters into CCN.

The exact mechanisms of the initial formation of clusters are very challenging to measure directly. Atmospheric H_2SO_4 concentrations are typically below 1 pptv (Riipinen et al., 2007), and the critical stabilizing agents may occur at even smaller or only slightly larger abundance. The initially forming clusters must have concentrations yet smaller than that. Also, the clusters contain only a few molecules, making them difficult to detect by many classical means, such as particle counters (e.g., Kulmala et al., 2012).

1.4 New particle formation in different parts of the atmosphere

New particle formation in the boundary layer has been observed in many different environments around the globe (e.g., O'Dowd et al., 2002; Kulmala et al., 2004c; Bae et al., 2010; Manninen et al., 2010; Shen et al., 2011; Hallar et al., 2011; Jung et al., 2013). Apparently, a wide variety of environments admits new particle formation. Therefore, it is plausible that it depends on the respective conditions, which compounds play an active role in actual ambient particle formation.

In addition to changes in conditions with geography, conditions also change markedly when going into the vertical. Air chemistry and temperature change, e.g., when ascending from inside a forest to the top of the canopy, to the top of the boundary layer, into the free troposphere (Seinfeld and Pandis, 2006). Indeed, formation of new particles has been observed in each part of the troposphere. Inside the boreal forest in southern Finland, new particle formation events have been frequently observed for many years (e.g., Kulmala and Kerminen, 2008). Above the boreal forest's canopy and throughout the boundary layer, airborne measurements could show that these new particle formation events extend throughout the boundary layer (e.g., O'Dowd et al., 2009). A confinement of new particle formation events to the boundary layer was observed at other locations as well (e.g., Crumeyrolle et al., 2010). However, new particle formation was also found to take place in the interface between the boundary layer and free troposphere (e.g. by measurements at high altitude: Venzac et al., 2008), as well as in the clean upper troposphere (e.g. by aircraft measurements: Clarke, 1993; Singh et al., 2002; Lee et al., 2003). Further observations of new particle formation in the free troposphere were made close to convective clouds (e.g., Weber et al., 2001;

Twohy et al., 2002). In most cases of free tropospheric particle formation, atmospheric dynamical processes are believed to locally create conditions favorable for new particle formation, such as decreases in coagulation and condensation sinks, increases in condensable vapor concentrations, or decreases in temperatures (e.g., Benson et al., 2008). For instance, concentrations of sulfur dioxide (SO_2) in the free troposphere can be substantially increased in convective outflows, leading to local enhancements of H_2SO_4 concentrations (Weigel et al., 2011). Similarly, boundary layer dynamics are believed to play a role in creating favorable conditions for particle formation, in particular during the break up of the nocturnal boundary layer during the morning time. Most experimental evidence thereof is provided by ground-based measurements (Nilsson et al., 2001; Pryor et al., 2011; Crippa et al., 2012), few from airborne measurements (Wehner et al., 2010).

In sum, direct airborne measurements of new particle formation are relatively rare (Clarke and Kapustin, 2010). They have rather delivered snapshots of hypothesized processes than been able to draw a consistent picture of how emissions, air chemistry, physical parameters and atmospheric dynamic processes contribute to the formation of particles in different parts of the atmosphere.

1.5 Objectives of this thesis

The main focus of this thesis lies on investigating the formation of new particles in the atmosphere by gas-phase precursors. Mainly, different experimental approaches were used to improve our understanding of this process. Carefully designed and controlled laboratory experiments were conducted to understand in how far classical nucleation theories can be applied to describe nucleation processes (**Paper I**), and to elucidate the mechanisms by which vapors initially form molecular clusters and new particles in the atmosphere (**Papers II–IV**). A correct and detailed knowledge of these mechanisms has been identified as important for improving global climate models (Carslaw et al., 2013). The laboratory studies were supported by ambient observations in the southern Finnish boreal forest. In addition, a newly commissioned platform for airborne aerosol measurements was described and successfully tested by conducting airborne measurements of ambient new particle formation events (**Paper V**). They are a first step in answering the call for a higher continuity of such measurements throughout all three dimensions of the atmosphere.

In detail, the aims of the thesis were:

1. To test classical heterogeneous nucleation theory and investigate limitations thereof when going towards small seed particle sizes; in particular to explore

the role of different materials for sub-10 nm seed particles in heterogeneous nucleation (**Paper I**).

2. To evaluate the applicability of a recently developed kinetic collision and evaporation model of cluster dynamics in comparison to direct measurements of ionic molecular clusters, in order to test the integrity of the measurements and to investigate electrically neutral clusters that can be simulated by the model but not yet measured (**Paper II**).
3. To try to reveal the exact mechanisms by which vapors initially form molecular clusters in the atmosphere by employing a novel mass spectrometer, able to directly measure ionic clusters, both in the field and during comprehensive measurement campaigns at a newly developed laboratory environment that is able to accurately simulate conditions relevant for atmospheric new particle formation. Particular emphasis lay on investigating the hypothesized important role of amines and oxidized organic compounds (**Papers III–IV**).
4. To map out in three dimensions where new particle formation occurs in the lower troposphere over the Finnish boreal forest, in particular during regional-scale particle formation events, by means of airborne measurements ranging from close to the forest canopy, throughout the boundary layer, and well into the free troposphere (**Paper V**).

2 Methods

2.1 Laboratory setups

2.1.1 The size analyzing nuclei counter (SANC)

The SANC is a powerful tool for investigating nucleation processes. Its chief asset is that it allows for very carefully chosen and well-known experimental conditions, and for fast and precise changes in the saturation ratio of the nucleating vapor $p_v/p_s(T)$. The SANC was used here to study the heterogeneous nucleation of n-propanol onto silver and salt seed particles (**Paper I**). The SANC is described in more detail, e.g., in Wagner et al. (2003). A schematic of the experimental setup for the SANC is presented in Fig. 1.

A considerable effort is made in creating well-defined experimental conditions (top half of Fig. 1). n-Propanol vapor is created by vaporizing the flow of liquid n-propanol originating from a syringe pump into a filtered and dried airflow by means of a micro orifice. This vaporization into the airflow occurs at 90 °C. Homogeneity of the vapor-

containing air is assured by passing it into a 50 L vessel, heated to 50 °C. Thereafter, the vapor-containing air mixes with the aerosol. The aerosol is created by flowing filtered and dried air or nitrogen over a salt or silver sample in a high-temperature tube furnace, and subsequently cooling the flow (Scheibel and Porstendörfer, 1983). Then, a radioactive source (^{241}Am) charges the aerosol, and a differential mobility analyzer (DMA) selects a monodisperse aerosol fraction (Reischl, 1991; Reischl et al., 1997). For our experiments, the geometric mean mobility-equivalent diameters of the selected aerosol fractions ranged from 4 to 12 nm. Subsequently, a second charger ("neutralizer") assures largely (> 90%) electrically neutral aerosol (Flagan, 1998; Fuchs, 1963). The aerosol is then mixed with the n-propanol/air mixture.

The flows into and out of the expansion chamber are remote-controlled using magnetic valves (bottom half of Fig. 1). Programmed cycles ensure that the valves open and close at exactly the right times. The aerosol sample is led into the expansion chamber and the expansion chamber subsequently sealed off. A sudden adiabatic expansion occurs when the expansion chamber is connected to a previously evacuated vessel by opening one of the magnetic valves. By this expansion, a rapid transition to a higher n-propanol saturation ratio is achieved. If the resulting saturation ratio is high enough, a part or all aerosol particles in the expansion chamber are activated by heterogeneous nucleation of n-propanol and subsequent growth to micrometer-size droplets. These droplets grow nearly simultaneously. Scattered laser light (wavelength 633 nm) is measured by a photomultiplier tube at a certain constant scattering angle (15°) in a continuous manner while the droplets grow to sizes of several µm. This method is called the constant-angle Mie scattering (CAMS) method (Wagner, 1985). It relies on the Mie solution of the Maxwell equations for light scattered by a sphere, which yields the light flux scattered at a certain angle as a function of the sphere's size (Fig. 2). A similar curve is produced experimentally as a function of time, when measuring the scattered light flux at the same angle during the growth of the ensemble of simultaneously growing droplets. By comparing that measured curve with the calculated curve, both the number concentration of activated droplets can be determined and the size of the growing droplets obtained as a function of time. For studying nucleation, the measurement of the droplet size versus time is incidental, but can be used to accurately (1–2%) verify the saturation ratio calculated from the expansion ratio and temperatures (Winkler et al., 2008b).

The main results of the measurements performed on the SANC for **Paper I** are the onset saturation ratios for activating particles of a certain size by the heterogeneous nucleation of n-propanol. The onset saturation ratio is the saturation ratio that activates just half of all particles of a certain size. It can also be calculated from Fletcher theory (Fletcher, 1958) and therefore be used to examine the validity of the classical theory of heterogeneous nucleation (Winkler et al., 2008a).

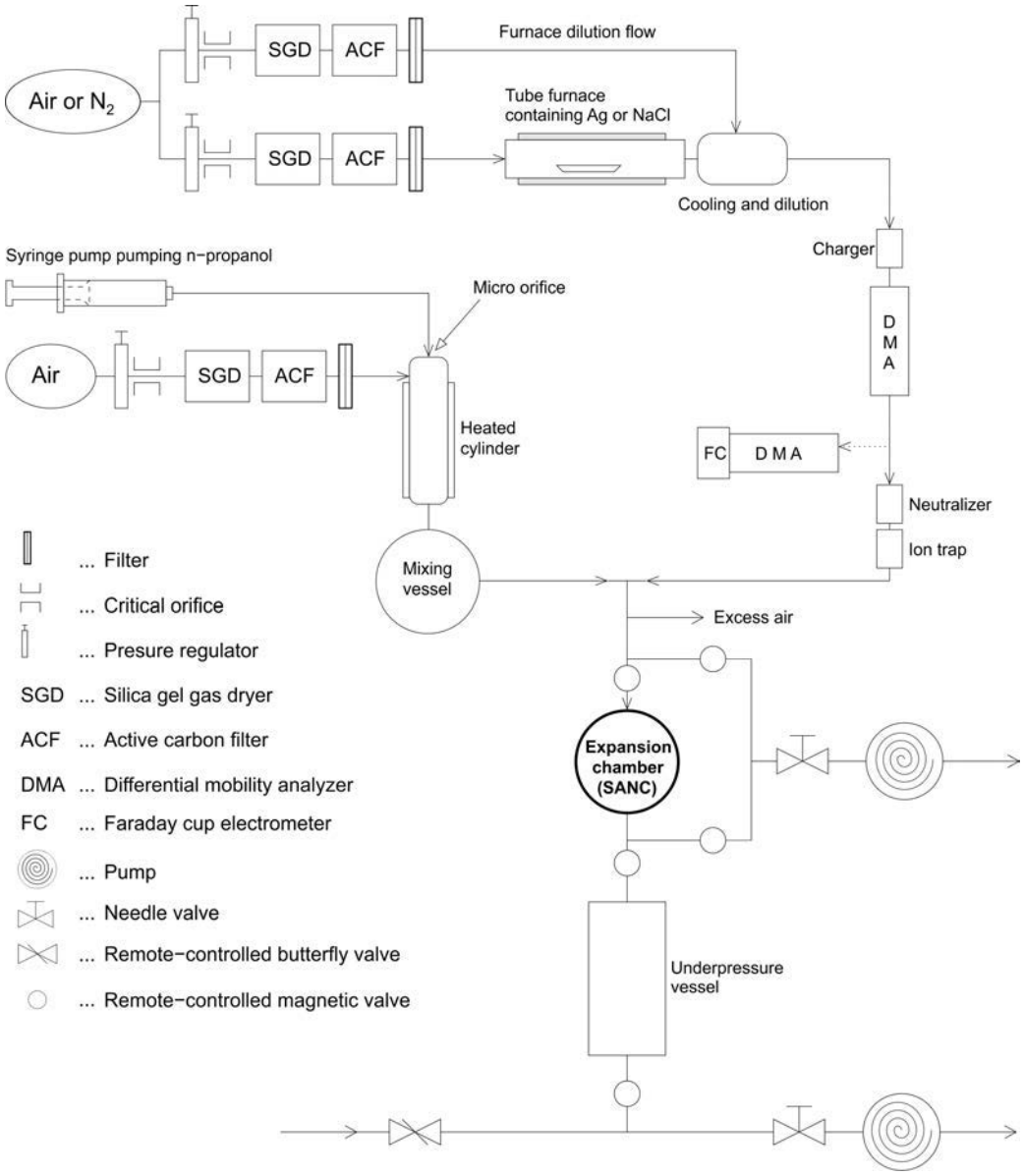

Figure 1: Slightly simplified schematic of the experimental setup for the size analyzing nuclei counter (SANC) (see also **Paper I**). The top half deals with the creation of a well-defined mixture of carrier gas (air), condensable vapor (n-propanol), and aerosol (silver, Ag, or salt, NaCl). The bottom half shows the system of remote-controlled magnetic valves that leads the sample into the expansion chamber. The valves subsequently create a rapid expansion in the expansion chamber by connecting it to the evacuated underpressure vessel.

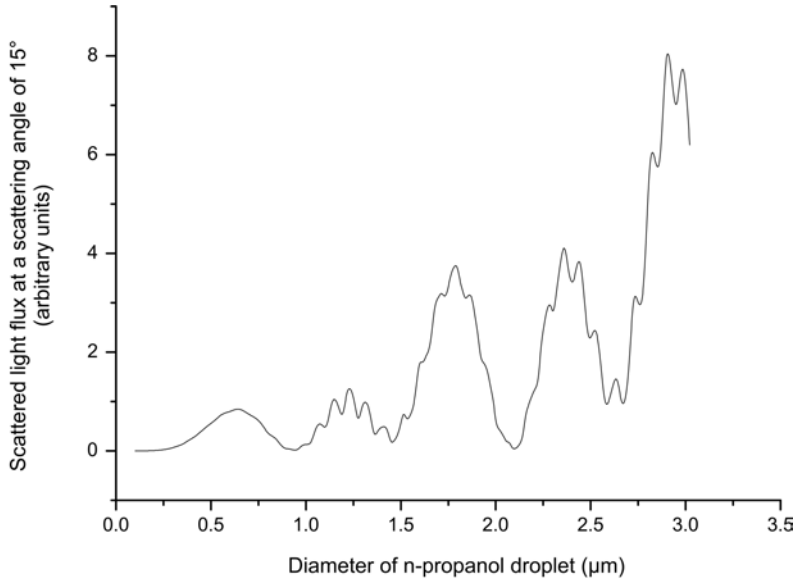

Figure 2: The light flux scattered from a spherical n-propanol droplet at a scattering angle of 15° versus the size of the droplet, calculated according to Mie theory. The light has a wavelength of 632.8 nm. A refractive index of 1.385 + 0i was used for n-propanol.

2.1.2 The CLOUD experiment

The "Cosmics Leaving Outdoor Droplets" (CLOUD) facility is located at the European Organization for Nuclear Research (CERN) close to Geneva, Switzerland. It is currently one of the most advanced laboratory environments to study the formation of aerosol particles from gas-phase precursors and their subsequent growth (Kirkby et al., 2011; **Papers III, IV**). It provides exceptionally clean and well-controlled experimental conditions. This cleanliness allows for studying particle formation and growth at atmospherically relevant, i.e. very low, concentrations of the participating vapors. In 2010 and 2011, three intensive measurement campaigns were run at the CLOUD facility, and results from these campaigns are an essential part of **Paper II**, and the chief contributions to **Paper III** and **Paper IV**.

The heart of the CLOUD facility is a cylindrical stainless-steel aerosol chamber of 26.1 m^3 inner volume, the CLOUD chamber. The setup is shown schematically in Fig. 3. A clean atmosphere is simulated inside this chamber by filling it with a mixture of air from cryogenic dewars (79% nitrogen, N_2, 21% oxygen, O_2), ozone (O_3) produced by UV irradiation, and de-ionized and purified H_2O that is added via a Nafion humidifier. In addition, trace gases can be added, each via a separate inlet line. SO_2 was almost always added as precursor for H_2SO_4. Other added trace gases, though usually not

added at the same time, were ammonia (NH_3), dimethylamine (C_2H_7N), and pinanediol ($C_{10}H_{18}O_2$). SO_2, NH_3 and dimethylamine were taken from gas bottles; pinanediol was evaporated from a solid reservoir. Air is fed continuously into the chamber at a total rate between 85 and 140 L/min. At the same time, a slightly smaller amount of air is extracted from the sum of all instruments sampling from the chamber, and the excess air is vented via an exhaust line, keeping the chamber fill slightly above atmospheric pressure to avoid contamination from outside.

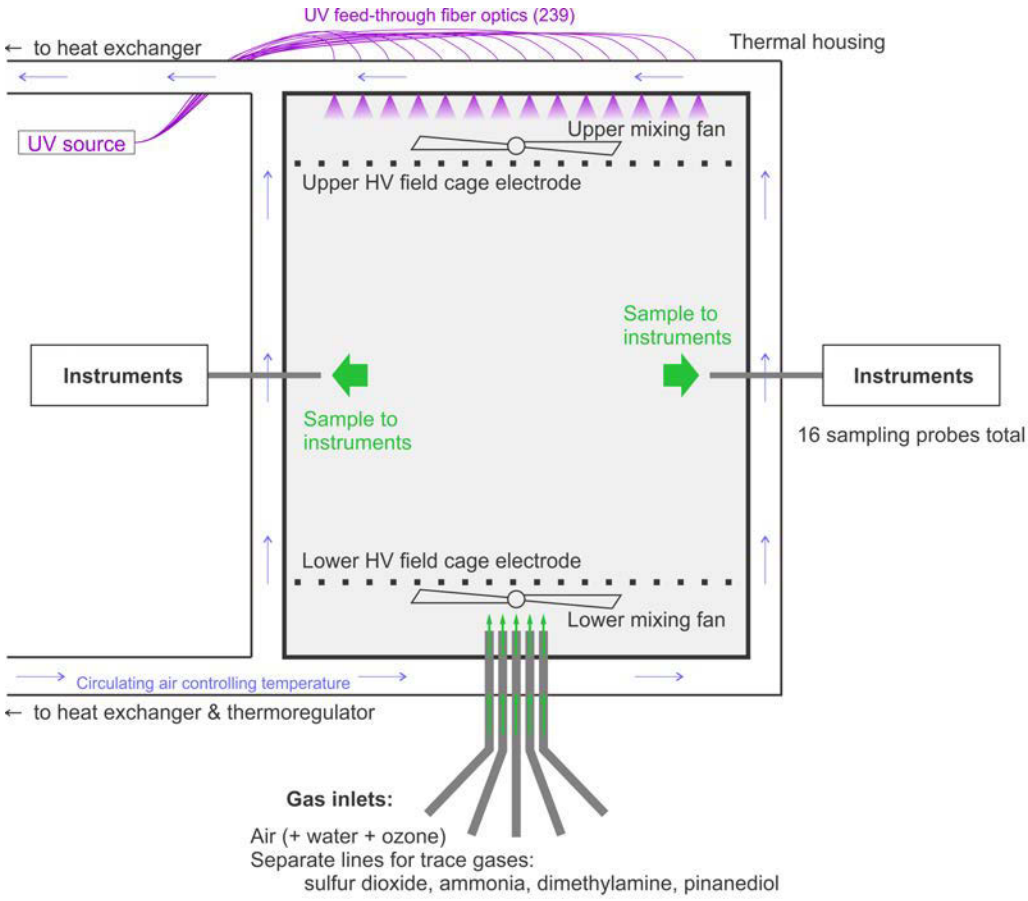

Figure 3: A schematic of the setup of the CLOUD facility at CERN. The CLOUD chamber, a stainless-steel cylinder of 3 m diameter and 26.1 m^3 inner volume, is shown with a gray shade. Clean air is obtained from cryogenic dewars and fed into the chamber from below the lower mixing fan, together with water, ozone and trace gases. Instruments are connected around the chamber at half height via 16 sampling ports that stick radially into the chamber.

The temperature of the chamber is regulated by a circulating airflow inside the chamber's thermal housing (Fig. 3). The thermal housing is insulating to the outside by layers of aluminum foil, rock wool and stainless steel sheets. This method keeps the temperature stable within 0.01 K for the time of a typical experiment. UV light can irradiate the inside of the chamber via an array of 239 optic fiber feedthroughs (Kupc et al., 2011). The UV light's purpose is to induce photolytic reactions to oxidize pinanediol and SO_2, the latter in order to obtain H_2SO_4 (Eisele and Tanner, 1993). One mixing fan each at the top and the bottom of the chamber ensure mixing in the chamber (Voigtländer et al., 2012). Ions inside the chamber are always created by background radiation, mainly galactic cosmic rays (GCR). The ion concentration can also be increased on demand, by exposing the chamber to a beam of pions (π^+) provided by the CERN Proton Synchrotron (Duplissy et al., 2010). Thereby, the mean total ion pair production rate in the chamber is adjustable, usually between 2.4 cm^{-3} s^{-1} and 45 cm^{-3} s^{-1}. In addition, all ions can be removed from the chamber by switching on a high-voltage (HV) electrical clearing field (20 kV m^{-1}) between a pair of field cage electrodes. The electrodes are mounted in front of the mixing fans at the top and the bottom of the chamber (Fig. 3).

Experiments at the CLOUD facility are performed during intensive measurement campaigns, typically lasting one to two months each. Together, the collaborating institutes provide a comprehensive suite of state-of-the-art instruments to sample and analyze the chamber contents. The instruments are arranged around the chamber and connected to it via 16 sampling probes, which are mounted radially around the chamber and extend 0.5 m (before 2011) or 0.35 m into the chamber.

Most important for this thesis, one or two atmospheric pressure interface time-of-flight mass spectrometers (APi-TOF; Junninen et al., 2010) were part of the instrumentation in each of the three campaigns during 2010 and 2011. They were used to measure the chemical composition of ions up to about 2 nm in mobility-equivalent diameter (for simplicity, henceforward all particle sizes are implicitly given in mobility-equivalent diameters). Ion number size distributions from 0.8 to 40 nm were measured by a neutral cluster and air ion spectrometer (AIS; Mirme et al., 2010). Aerosol size distribution measurements covered the range from 1.3 to 100 nm. They were performed by a scanning mobility particle sizer (Wang and Flagan, 1990) for the size range of 10–100 nm, together with an array of condensation particle counters with different cut-off sizes, including novel diethylene glycol-based counters (Iida et al., 2009) such as the particle size magnifier (PSM; Vanhanen et al., 2011). This instrumentation allowed for determining formation rates of particles in the CLOUD chamber from 10^{-3} to $>10^2$ cm^{-3} s^{-1} (**Papers III–IV**), as well as particle growth rates (Kulmala et al., 2012; 2013). Crucially important were also the measurements of the relatively low gas-phase concentrations of critical compounds. Concentrations of H_2SO_4 were measured down to

10^5 cm^{-3} by means of a chemical ionization mass spectrometer (CIMS; Kürten et al., 2011, 2012). Concentrations of NH_3 were measured down to 35 pptv (until 2011) or 0.2–3.7 pptv (in 2012) by using a proton transfer reaction mass spectrometer (PTR-MS; Norman et al., 2007), and a long path absorption photometer (LOPAP; Bianchi et al., 2012) or an ion chromatography setup (IC; Praplan et al., 2012). The IC also measured concentrations of dimetylamine down to 0.2–1 pptv. In 2011, the PTR-MS was adapted to measure concentrations of pinanediol down to 5 pptv.

Most experiments at the CLOUD chamber were performed at a temperature of 5 °C and a relative humidity of 38% to 41%. All reported results were obtained at these conditions, unless noted otherwise.

2.2 Measurement devices

2.2.1 Condensation particle counters (CPCs)

A condensation particle counter (CPC) is an instrument that counts aerosol particles by growing them into detectable droplets. (As such, the SANC described in section 2.1.1 is also a large CPC.)

The ability to measure low concentrations of small particles at high precision has long been in high demand in experimental aerosol research. CPCs have been developed and used for more than 100 years (Aitken, 1889; McMurry, 2000). Current commercial CPCs are commonly able to count single particles down to 3 nm at a time resolution of 1 s. In addition, they are compact (< 30 L), light (< 10 kg), and fairly easy to use and maintain. As a result, they have become the workhorse of aerosol research. They measure aerosol particle number concentrations at a high time resolution, which can be used to measure formation rates (Kulmala et al., 2012; **Paper III**), and they are used as particle detectors in size-resolving measurement setups (e.g., Wang and Flagan, 1990). Batteries of differently operating CPCs have been used to investigate particle growth rates, as well as chemical properties (Kulmala et al., 2007; Riipinen et al., 2009).

Most commercially available CPCs are of the laminar flow type. In the most common types of this instrument, the sample is first saturated with n-butanol vapor at a warm temperature (e.g., 40 °C). Thereafter, the sample is cooled (e.g., down to 10 °C), which creates a high enough supersaturation of the n-butanol vapor to condense onto the aerosol particles. Each thereby activated aerosol particles grows into an n-butanol droplet of about 10 µm, which is then counted optically (McMurry, 2000).

More recently, CPCs have been developed that use diethylene glycol as working fluid (Iida et al., 2009). These are either of the laminar flow type (Wimmer et al., 2013), or the mixing type. In the latter type, supersaturation is achieved by turbulently mixing a

hot saturated flow with a cold sample flow. These CPCs can obtain a cut-off size of down to 1.05 nm (Vanhanen et al., 2011).

2.2.2 The atmospheric pressure interface time-of-flight mass spectrometer (APi-TOF)

APi-TOF mass spectrometers were used to study the composition of ions and ionic molecular clusters during new-particle formation experiments. The results from the measurements using APi-TOFs at the CLOUD chamber are a major part of this thesis (**Papers II–IV**). The functioning of the APi-TOF and its capabilities were first described by Junninen et al. (2010) and Ehn et al. (2010).

2.2.2.1 Measurement principles

For this thesis, no dedicated ionization of the sample was performed. Therefore, the APi-TOF was always used to detect ions already charged before being sampled, i.e., in the actual atmosphere or in the simulated atmosphere inside a chamber. Only either positively or negatively charged ions can be measured at a given time.

A schematic of the APi-TOF's operation is presented in Fig. 4. Usually, sample is drawn to the instrument's inlet mainly by a pump-driven make-up flow at a total flow rate of 5–10 L/min. 0.8 L/min enter the instrument via a critical orifice (diameter 0.3 mm), sucked in by the vacuum inside the instrument. A series of ion guiding elements focuses the ions and guides them to the time-of-flight side of the instrument (TOF), whereas air is pumped away by a scroll pump and a differentially pumping turbo pump. These pumps provide a vacuum that is step-wise increasing towards the TOF, where the pressure is 10^{-6} mbar. Electrical fields in the TOF send the ions onto a flight path to a multichannel plate ion detector. The time-of-flight of an ion is a function of its mass-to-charge ratio (m/z).

The APi-TOF measures the mass-to-charge ratio (m/z) of the ions and ionic clusters, expressed in units of thomson (Th), at an accuracy of < 10 ppm. The resolving power is usually around 5000 Th/Th. The range of m/z for ions to be detected can be adjusted by tuning the APi-TOF's ion guiding elements and adjusting the duty cycle period. Also dependent on this tuning is the transmission efficiency, i.e., the fraction of actually detected ions out of all the ions reaching the APi-TOF's inlet (Ehn et al., 2011). For most measurements performed for this thesis, the detectable m/z range was from 50 to 3300 Th. Only singly charged ions were detected, so this range corresponds to 50 to 3300 unified atomic mass units (u) or dalton (Da). As a comparison to classical aerosol measurements, 3300 Da correspond to about 2.1 nm when converted to mobility equivalent diameter using the bulk density of ammonium bisulfate (Ehn et al., 2011).

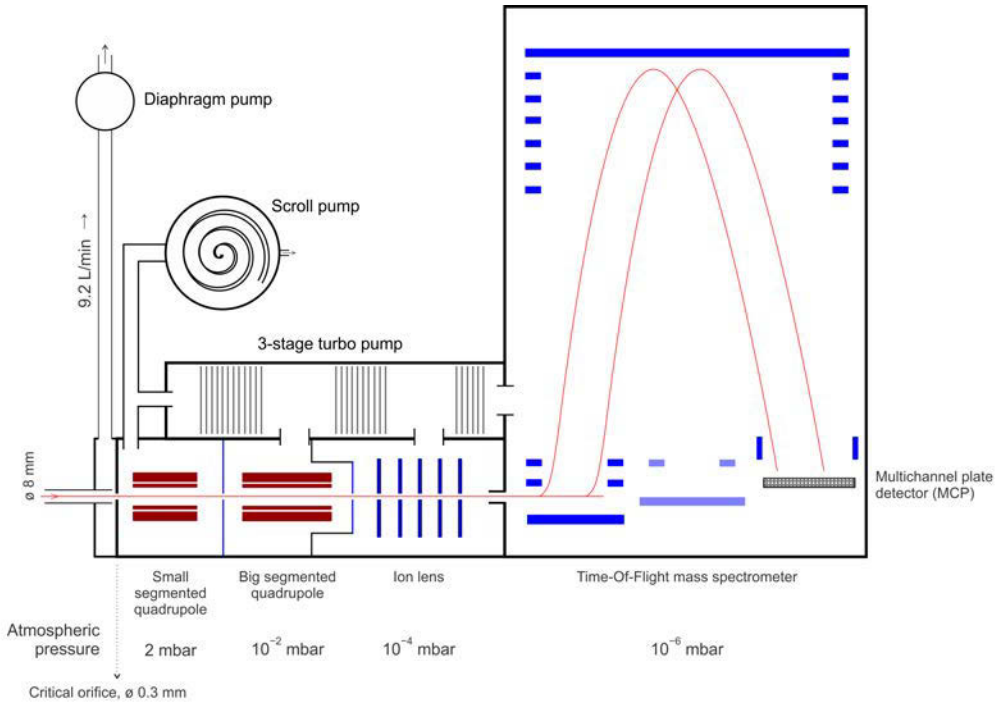

Figure 4: Schematic of an atmospheric pressure interface time-of-flight mass spectrometer (APi-TOF) in operation. To the left, gas is usually at atmospheric pressure and is drawn to the instrument at a total flow of 10 L/min (for most operations at the CLOUD experiment). 9.2 L/min are make-up flow, the remaining 0.8 L/min get sucked into the instrument through the critical orifice by the vacuum inside the instrument. The red lines show simplified trajectories of the sampled ions. They are focused and guided to the time-of-flight mass spectrometer and eventually detected when hitting a multichannel plate.

2.2.2.2 Fragmentation of ion clusters inside the APi-TOF

In order to measure ion clusters, it is important that such clusters are not fragmented during the measurement process. One cause of fragmentation can be the low pressure inside the APi-TOF, which enhances any evaporation of molecules. However, the time an ion cluster is exposed to this low pressure is only a few µs, so only weakly bound molecules have enough time to evaporate. Such a weakly bound molecule would require gas-phase concentrations of its kind of at least 1 ppmv at ambient pressure, so that it would be in the cluster in equilibrium conditions. At the CLOUD experiment, the only vapor present at these concentrations is H_2O. Indeed, with a few exceptions, no H_2O is found bound to ion clusters in most experimental conditions. In particular

clusters containing mainly sulfuric acid are almost always observed without any H_2O attached, although they are assumed to be stabilized also by H_2O molecules in ambient conditions (Vehkamäki et al., 2002; Yu, 2006). Some hydrated sulfuric acid ions and ion clusters are detected by the APi-TOF at conditions of high humidity (>60%, 19 °C). But these are probably remains from the condensation of H_2O molecules during the adiabatic expansion of the sample that occurs when the sample enters the instrument via the critical orifice.

A more important cause of fragmentation of ion clusters is the acceleration that the ions experience by the electrical field of the ion guiding elements in the APi-TOF (e.g., quadrupoles and ion lenses). The acceleration leads to gas–ion collisions with higher energy than those expected thermodynamically according to the Maxwell-Boltzmann distribution (Jennings, 1968; de Hoffmann and Stroobant, 2007). The probability that a certain ion cluster fragments due to such collisions is difficult to calculate as well as to measure. Our observations show that many molecular clusters, up to 3300 Th and larger, can be detected (**Papers II-IV**). Comparisons of the APi-TOF results with the less disturbing measurements by ion mobility spectrometers also show good agreements. So the detected ions and ion clusters are in general representative of the measured ion number size distribution (Ehn et al., 2011; **Paper IV**). However, results from quantum-chemistry-based calculations suggest that partial fragmentation does occur in the form of the loss of one or two molecules from certain ion clusters (**Papers II, III**).

2.2.2.3 Data analysis

The elemental composition of ions is determined primarily from their exact mass. For each element, the exact mass is slightly different from the integer ("nominal") mass, the latter being defined as 1/12 the mass of a ^{12}C atom times the total number of protons and neutrons. The difference is due to the element's nuclear binding energy, and also called the mass defect. An ion of a certain elemental composition has a unique mass defect and exact mass, which is measured by the APi-TOF and used to identify this composition. E.g., the nominal mass of the bisulfate ion HSO_4^- is 97 Da and its exact mass is 96.9601 Da. Therefore its mass defect is –0.0399 Da.

A secondary means of identifying an elemental composition is the distinctive pattern it creates in a mass spectrum due to the natural abundances of the elements. E.g., for the signal from the ion cluster $(H_2SO_4)_3 \bullet HSO_4^-$, 78% are expected, and indeed measured, at *m/z* 391, 17% at *m/z* 393, 3% at *m/z* 392, 1.5% at *m/z* 395, and the remaining signal at *m/z* 394, 396 and 397 (Fig. 5).

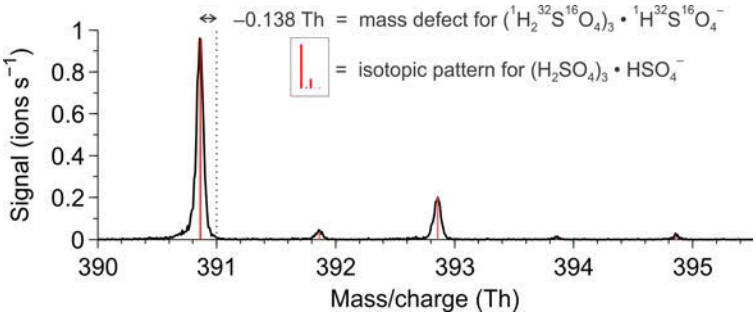

Figure 5: Sample section from an APi-TOF mass spectrum of negatively charged ions. Illustrated are the methods used for identifying the signal (shown as black line) as the sulfuric acid tetramer anion cluster $(H_2SO_4)_3 \bullet HSO_4^-$. Shown in red is the isotopic pattern for this ion cluster, which results from calculating the exact masses of all the cluster's isotopes.

In practice of course, the APi-TOF's limited accuracy and resolving power (see section 2.2.2.1) and limited signal-to-noise set limits to how unambiguously an elemental composition can be determined. E.g., for **Paper IV**, O_2 (31.99 Da) could be distinguished from S (31.97 Da) only up to about *m/z* 700.

Note that these methods only allow for determining elemental compositions from the APi-TOF measurements, but not the configuration of the atoms. E.g., the data shown in Fig. 5 can be unambiguously assigned to the elemental composition $H_7S_4O_{16}^-$, but their identity with the sulfuric acid tetramer anion $(H_2SO_4)_3 \bullet HSO_4^-$ has to be inferred.

The raw data from the APi-TOF consists of spectra of ion counts versus time-of-flight, with usually more than 10^5 data points per spectrum. Spectra can be recorded at a rate of > 10 kHz. Therefore, a substantial amount of data processing is required; firstly to obtain a reasonable amount of mass spectra, each with an accurately calibrated mass axis, and secondly to extract the desired scientific information. APi-TOF data obtained for this thesis were processed and analyzed using tofTools, a software package based on MATLAB and under continuing development, mainly at the University of Helsinki (Junninen et al., AMT, 2010). More detailed descriptions of how current versions of tofTools can be used are given in Ehn et al. (ACP, 2012) and the supporting information of **Paper IV**.

The data processing involves at least four main steps: Step 1, averaging the raw data in time; step 2, converting from time-of-flight to *m/z* (= mass calibration); step 3, identifying elemental compositions; step 4, extracting actual counts for identified and unidentified compounds. Step 1 reduces the amount of spectra to deal with and increases the signal-to-noise, at the cost of time resolution. Step 2 is critical because step 3 relies on an accurate mass calibration. In most cases, one can achieve a mass

calibration resulting in deviations < 10 ppm by converting time-of-flight *t* to *m/z* according to

$$\frac{m}{z} = \left(\frac{t-b}{a}\right)^{p} \quad [4]$$

where *a*, *b* and *p* are free parameters for fitting at least four pairs of measured *t* and calculated *m/z* (= calibration peaks; Ehn et al., 2012). Therefore, at least four peaks in the spectrum have to be from ions of known compositions. Experience and a satisfactory mass calibration serve as strong indicators that the initial *a priori* attributions of compositions to peaks have been adequate. Care has to be taken that the calibration peaks cover a large part of the *m/z* range of interest to assure that the fit is good at all *m/z* of interest. Therefore it can be necessary to iterate steps 2 and 3 to accordingly extend the set of calibration peaks.

Fig. 6 illustrates steps 3 and 4 by showing essentially the same section of a mass spectrum as in Fig. 5, but for a different experiment, resulting in a different, more complex result.

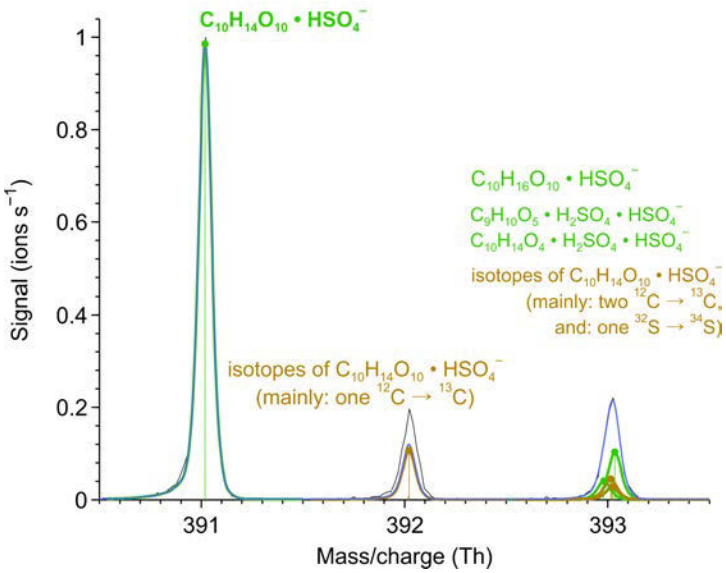

Figure 6: Section from an APi-TOF mass spectrum, to illustrate part of the data analysis process. The figure is adapted from the supporting information of **Paper IV**. The measured signal is shown as black line. Likely identified compounds, used for explaining the signal, are shown in green (primary isotopes) and in brown (secondary isotopes, dependent on the primary isotopes). Labels explain the identified elemental composition. Vertical lines mark their masses; thick green and brown lines are fits. The blue line is the sum of all fits, which is optimized to fit the black line.

The peak at *m/z* 391 is identified as $C_{10}H_{14}O_{10} \bullet HSO_4^-$ and the signal is fitted by adjusting the height of the peak of the compound's primary isotope, taking into account the previously determined peak shape. Additional compounds are then identified at *m/z* 393 and fitted, taking into account isotopes of $C_{10}H_{14}O_{10} \bullet HSO_4^-$ that have similar masses. The application of this procedure to the whole spectrum yields a so-called peak list, consisting of all identified compositions (step 3). Step 4 usually consists of extending this peak list, so that it also includes unattributed signal, and then fitting the whole spectrum.

2.3 Atmospheric observations

2.3.1 Using a Cessna 172 as an airborne measurement platform

Most results reported on in **Paper V** are from measurements taken by an airborne measurement platform. The aircraft is a Cessna FR172F single-engine airplane. Pilot and scientist sit next to each other; most instruments are built into a rack behind them. Sample air is collected from the undisturbed airflow ahead of the aircraft's right wing, using an inlet designed specifically for sampling aerosol from an airplane (McNaughton et al., 2007). The sample is transported to the instruments in the cabin at a high flow rate of 50 L/min to minimize losses of aerosol particles. Afterwards, the sampled air exits through a venturi, which is mounted on the right main gear leg. The suction in the venturi, the aircraft's forward movement and a manual valve, operated from the co-pilot's seat, maintain a constant total sampling flow of 50 L/min. Pumps inside the instruments and one external pump assure the correct inlet flows for each instrument in the rack. Fig. 7 depicts the arrangement of instruments and air flows.

For most flights during 2009, the instruments in the rack were: a CO_2/H_2O analyzer (LI-COR LI-840), a "CPC battery" consisting of three CPCs tuned for cut-off sizes of 3, 6 and 10 nm (TSI models 3776 and 3772), a triple-wavelength particle/soot absorption photometer (PSAP, Radiance Research), and a single-wavelength integrating nephelometer (Radiance Research Model 903). The TSI 3772 CPCs (6 and 10 nm cut-off sizes) were optionally equipped with a dilution system with a dilution factor of 1:10. Dilution was necessary for measurements of high aerosol particle number concentrations, e.g., when measuring industrial or biomass burning plumes. The main results for **Paper V** were obtained from the CPC battery. It measured at a time resolution of 1 s, which translates to a spatial resolution of 35 m due to the aircraft's speed. For flights in 2010, the CPCs with 6 and 10 nm cut-off sizes were replaced by a scanning mobility particle sizer (SMPS; Wang and Flagan, 1990), measuring the

particle size distribution from 10 to 350 nm at a time resolution of 2.1 minutes, translating to a spatial resolution of 4.5 km. Further equipment was a sensor to measure temperature and relative humidity (Thomas 107CDC20/12), which was attached to the air inlet on the right wing, a GPS receiver, and a computer to collect all data and monitor the measurements during the flight. During 2010, a web camera was installed as well to visually record weather and cloud conditions.

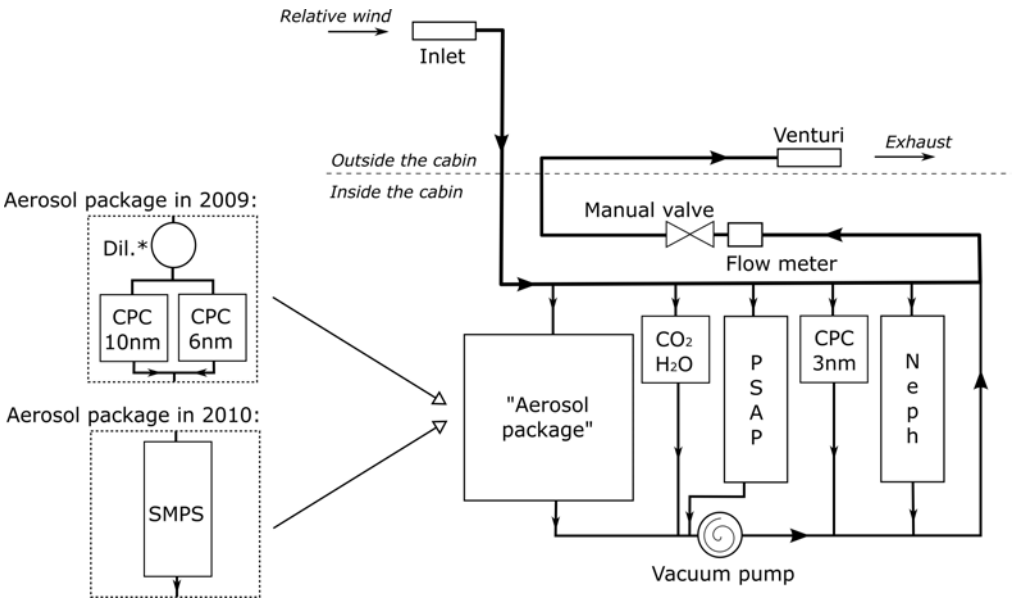

Figure 7: A schematic depiction of the sampling setup used onboard the Cessna FR172F airborne measurement platform (from **Paper V**), and an overview of the instrumentation inside the aircraft's cabin. The aircraft is flying from the right to the left. The sample air enters through the inlet, which is mounted under the right wing and exits through a venturi, mounted on the right main gear leg. Flow meter and valve are located at the co-pilot's seat, the instruments in a rack behind the seats. "Dil.*" is an optional dilution system (dilution factor 1:10).

2.3.2 Station for measuring ecosystem-atmosphere relations (SMEAR)

Comprehensive measurements on ecosystem and atmosphere have been made at the Finnish SMEAR stations for many years. The most comprehensive one today is the SMEAR II station (Hari and Kulmala, 2005; Hari et al., 2009). It is situated at a fairly remote site, in Hyytiälä, Finland, inside a boreal forest. The surrounding trees consist mainly of Scots pine (*Pinus sylvestris* L.). The closest larger town is Tampere, 50–60 km southwest of the station.

A host of atmospheric observations have been made at the SMEAR II station continuously since 1996, including extensive aerosol measurements (Kulmala et al., 2004b). In particular, measurements by the differential mobility particle sizer (DMPS; Aalto et al., 2001), ion mobility spectrometers, such as the AIS (Manninen et al., 2009), and CPCs are used to detect and analyze new particle formation events. Measurements from the SMEAR II station's DMPS are the principal ambient data used as comparison with the results from the airborne measurements in **Paper V**. In **Paper IV**, APi-TOF measurements made at the CLOUD facility at CERN were compared with ambient observations made by the same APi-TOF at the SMEAR II station. The availability of supporting routine measurements at the SMEAR II station turned out crucial for a complete interpretation of the results and their atmospheric implications.

3 Mechanisms of nucleation and new particle formation: Review and results of this thesis

3.1 To the limits of heterogeneous nucleation theory

Classical nucleation theory has the advantage over many more modern methods that it can be applied easily to predict the nucleation behavior of vapors: calculations are fast to compute, and only some basic thermodynamic data is needed as input. Problems are that these thermodynamic data are often not available or inaccurate, and that calculated nucleation rates may differ from actual experimental results by orders of magnitude (Vehkamäki, 2006). However, the dependencies of nucleation rates on temperature and on the saturation ratio of the condensing vapor(s) are often predicted well (e.g., Wölk and Strey, 2001; Gaman et al., 2005). Saturation ratios required for obtaining a certain substantial rate of homogeneous nucleation can be predicted fairly successfully as well (e.g., Viisanen et al., 1994). The corresponding item in the case of heterogeneous nucleation is the saturation ratio necessary to activate a seed particle. The fraction of activated seed particles, the activation probability, shows a sharp transition from 0 to 1 with increasing saturation ratio (given a monodisperse seed aerosol). The defining measure of this transition is the onset saturation ratio, i.e., the saturation ratio that activates 50% of the seed particles.

The application of classical nucleation theory to calculate the onset saturation ratio is known as the Fletcher theory (Fletcher, 1958). Fletcher theory can work very well down to very small sizes of seed particles. E.g., the measured onset saturation ratios agree very well with Fletcher theory for the activation of tungsten oxide (WO_x) particles by n-propanol for particle diameters down to 1.5 nm (Winkler et al., 2008a). Moreover, the size of the critical cluster of a droplet nucleating on single ion molecules (~1.5 nm) can

be determined from similar measurements and by using the heterogeneous nucleation theorem (Vehkamäki et al., 2007; Winkler et al., 2012). Again, the results agree well with r^* in the classical Kelvin-Thomson equation (i.e., Eq. 2, with an additional term to account for the charge of the seed particle).

These successes of classical nucleation theory down to the molecular level may be surprising, as it relies on macroscopic properties such as surface tension and density. Classical nucleation theory apparently performs well in predicting the behavior of at least certain combinations of seed particles and condensing vapor. However, it performs worse for other combinations. E.g., Petersen et al. (2001) found an unexpectedly high onset saturation ratio necessary for activating 7 nm salt (NaCl) seed particles by n-propanol at 15 °C. Subsequently, we found more unexpected behavior, when we systematically studied the heterogeneous nucleation of n-propanol vapor on 4 to 11 nm NaCl seed particles (**Paper I**) at temperatures ranging from –11 to +14 °C. Not only is the onset saturation ratio at 14 or 15 °C higher than expected, but the temperature dependence is reversed: Nucleation occurs at lower saturation ratios at lower temperatures and vice versa, whereas the opposite is expected from Eq. 2, and consequently from Fletcher theory (Fig. 8). Fletcher theory takes into account the interaction between the vapor and the seed particle in terms of the contact angle Θ. It is the macroscopic angle between the gas-liquid interface of the condensing vapor and the liquid-solid interface between the condensing vapor and the seed particle. The value for Θ has a strong influence on the saturation ratio required for activation, which increases with increasing Θ (Fletcher, 1958). Theoretically therefore, a temperature-dependent contact angle would result in a reversal of the observed temperature dependence of the onset saturation ratio. However, there is no reason to expect such a behavior of Θ. And indeed, measurements of Θ for n-propanol in NaCl result in $\Theta = 0$ for all investigated temperatures, from –7 to +30 °C (**Paper I**).

It seems that the classical nucleation theory, which is based on macroscopic properties, fails to adequately describe the nucleation of n-propanol on NaCl seed particles, at least below sizes of 11 nm. On the other hand, control measurements with silver particles instead of NaCl particles brought the expected qualitative results (**Paper I**), and quantitative agreement is achieved for the case of silver particles when an additional macroscopic effect, line tension, is taken into account (Hienola et al., 2007; Winkler et al., 2008b). Another observation was the shrinkage of furnace-generated aerosol particles of up to 16% when brought in contact with of n-propanol vapor, which occurs for NaCl particles, but not for silver particles (**Paper I**). We can hypothesize that an explanation for these phenomena lies in the microscopic properties of the involved vapors and seed particle materials and in molecular-scale interactions between them.

n-Propanol is a polar molecule, and NaCl is a crystal, i.e., a lattice of ions, whereas silver is a metal. Indeed, the shrinkage of NaCl particles is very likely due to

microstructural rearrangements that are induced by a polar vapor. Such shrinkage was shown to also occur in the presence of water, i.e. another polar vapor, for particles sizes of 6–144 nm (Krämer et al., 2000; Biskos et al., 2006). NaCl aerosol particles created by condensation are known to have chain-like microstructures (Craig and McIntosh, 1952), which are probably restructured into more compact agglomerates by adsorbed polar molecules. Shrinkage was also observed for ammonium sulfate particles in the presence of water (Mikhailov et al., 2009). These observations suggest that microstructural rearrangements of particles formed by condensation are a general property of combinations of salt particles and polar vapors.

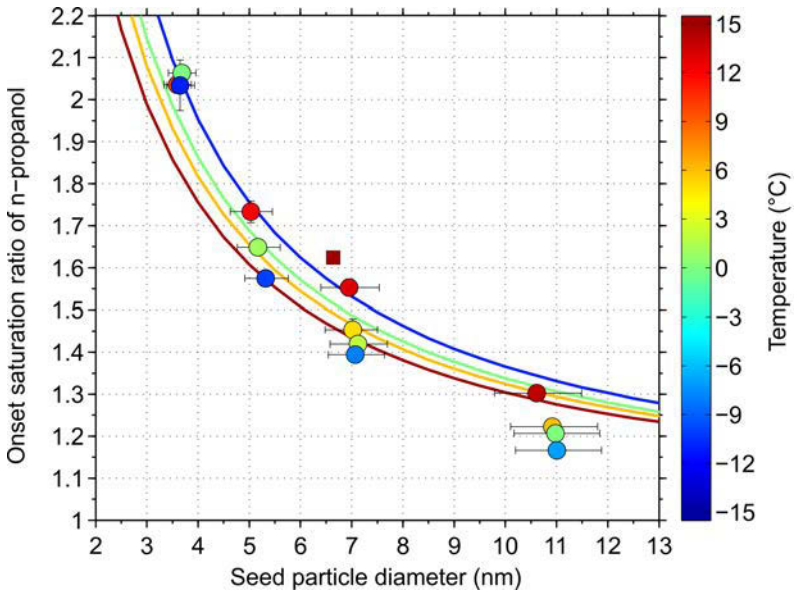

Figure 8: Onset saturation ratio of n-propanol to activate NaCl seed particles, plotted versus seed particle diameter. Adapted from **Paper I**. Temperatures vary between –11 and +14 °C (color-coded). Circles are experimental results; vertical error bars represent measurement uncertainties, horizontal error bars the geometric standard deviation of the monodisperse seed aerosol, resulting from the width of the DMA transfer function. The square shows the earlier result by Petersen et al. (2001), which motivated these measurements. Predictions according to Fletcher theory are shown as lines.

The reversed temperature dependence of activation probabilities hints at interactions between condensing polar n-propanol molecules and the NaCl particle that become more attractive (or less distractive) with decreasing temperatures.

There have been attempts at addressing molecular-scale interactions in nucleation phenomena theoretically, resulting in the expected departures from classical theory for

the calculated saturation ratios, in both homogeneous and heterogeneous nucleation (e.g., McGraw et al., 2012). However, knowledge of the specific molecular interactions among the participating vapors and seed particles will anyway be required. Already below 10 nm, the microphysical and chemical properties of surfaces and molecules can become crucial, as seen from the results in **Paper I**.

Nucleation as a source of newly formed aerosol particles in the atmosphere involves even much smaller sizes. The initial steps of new particle formation in the atmosphere occur below 2 nm (Kulmala et al., 2013). It seems likely that additional theoretical approaches and correspondingly novel experimental techniques are needed, if we are to understand the underlying mechanisms of these processes.

3.2 Understanding the formation of clusters by mass spectrometry and quantum chemistry

3.2.1 Effect of electric charge and NH_3 on the formation of H_2SO_4 clusters

Gaseous H_2SO_4 is produced quickly in the atmosphere by solar radiation, following the photo-oxidation of atmospheric SO_2 by OH to HSO_3 (Eisele and Tanner, 1993). H_2SO_4 is lowly volatile and indeed routinely observed in atmospheric aerosol (Vehkamäki et al., 2002; Jimenez et al., 2009). Also, observed particle formation rates scale as $[H_2SO_4]^{1–2}$ (e.g., Weber et al., 1996; Sihto et al., 2006), indicative of photo-oxidation processes playing an important role in particle formation. Therefore, it is widely believed that H_2SO_4 is involved in the formation of new particles in the atmosphere. The question remains exactly which other compounds contribute and how. Very likely, the first step of new particle formation involves the formation of small stable clusters involving H_2SO_4 molecules (e.g., Sipilä et al., 2010; Petäjä et al., 2011). Water molecules (H_2O) are well known for their stabilizing effect on H_2SO_4, and binary homogeneous nucleation of H_2SO_4 and H_2O is assumed to be an important source of newly formed particles in the upper troposphere (Hegg et al., 1990; Weber et al., 1999; Vehkamäki et al., 2002). Due to their relative abundance (typically 10^{15} to 10^{18} $cm^{–3}$, i.e. many orders of magnitude higher than $[H_2SO_4]$), H_2O molecules can always be involved in stabilizing H_2SO_4 clusters. More effective stabilizing agents that have been suggested for a long time are electrical charge (e.g., Raes and Janssens, 1985; Lovejoy et al., 2004) and NH_3 molecules (e.g., Coffman and Hegg, 1995; Kulmala et al., 2000). From the point-of-view of the classical theories, electric charge is favorable for nucleation, because the electrostatic interactions between the ion and other molecules lower the Gibbs free energy barrier to be overcome for forming a critical cluster (“ion-induced nucleation”). NH_3 is a candidate, because it is present in the gas-phase, often in concentrations exceeding those of H_2SO_4. As a base, NH_3 can form salts with acids

such as H_2SO_4 that have much lower volatility, and it was shown to reduce the saturation vapor pressure of H_2SO_4 in bulk H_2SO_4-H_2O solutions by several orders of magnitude (Marti et al., 1997). More recently, quantum chemical ab-initio studies have also shown a stabilizing effect of NH_3 on H_2SO_4 clusters by the formation of bonds, stronger than that of water (Kurtén et al., 2007; Ortega et al., 2008). In detail, the binding of NH_3 to H_2SO_4 is facilitated by hydrogen bonds.

Consequently in 2010, the first campaigns at the CLOUD facility ("CLOUD campaigns") focused on studying new particle formation in the binary H_2O-H_2SO_4 and in the ternary NH_3-H_2O-H_2SO_4 system, plus investigating the effects of electric charge. An APi-TOF was among the novel experimental techniques employed. The results from these experiments showed that electrically neutral particle formation from only H_2O and H_2SO_4 requires about two orders of magnitude higher concentrations of H_2SO_4 than found in ambient observations to obtain comparable formation rates (Kirkby et al., 2011). Including the ion-induced formation pathway, or adding NH_3, or both, all enhance the formation rates, but they still always fall short of the expectations from ambient observations (Kuang et al., 2008; Kerminen et al., 2010). Significant particle formation rates at ambient levels of H_2SO_4 were only obtainable for low temperatures (–25 °C). The enhancement achievable by including ions or NH_3 was again noticeable. As predicted therefore, the binary or ternary (NH_3-)H_2O-H_2SO_4 system can account for new particle formation in colder regions, such as in the free troposphere (Kirkby et al., 2011). Furthermore, particle formation in the boundary layer that includes other compounds may still also involve NH_3, as well as ions, both with noticeable effects. Therefore, particle formation from NH_3, H_2O and H_2SO_4 deserves a closer look.

The APi-TOF performed exceptionally well at the CLOUD experiments, allowing for the chemical identification of practically all ions and ion clusters. This success is mainly due to the extraordinary level of cleanliness that the CLOUD facility achieves. Thus, less ion signal is "wasted" on compounds that we are not interested in. The total ion signal is further enhanced due to the substantial augmentation of the ion pair production rate in the CLOUD chamber when using the π^+ beam provided by CERN's Proton Synchrotron.

The results obtained from the APi-TOF reveal the details of new particle formation in the CLOUD chamber for the NH_3-H_2O-H_2SO_4 system; by directly measuring the composition of the growing negatively and positively charged clusters (Figs. 9, 10). These clusters are in general $(NH_3)_m \bullet (H_2SO_4)_n \bullet HSO_4^-$ and $(NH_3)_m \bullet (H_2SO_4)_n \bullet NH_4^+$, respectively. No H_2O is observed in these clusters, as these molecules are too loosely bound to remain in the clusters during the sampling by the APi-TOF (see section 2.2.2.2).

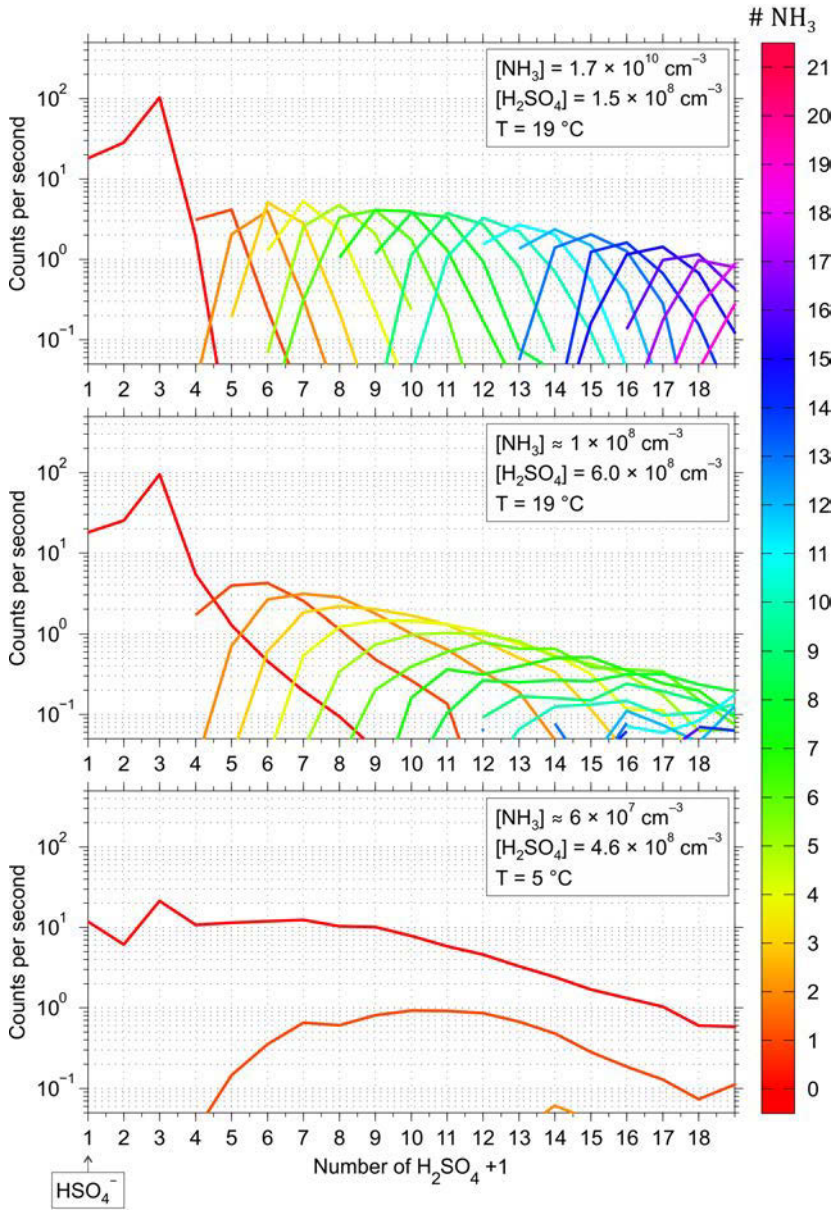

Figure 9: A summary of the majority of anion signal obtained by the APi-TOF at CLOUD during three different new particle formation experiments with NH_3, H_2O and H_2SO_4. Shown are ion counts vs. number of H_2SO_4 molecules in the clusters, including a bisulfate (HSO_4^-) ion. Colors reveal the amount of NH_3 molecules in each cluster. Therefore, the clusters' composition is $(NH_3)_m \bullet (H_2SO_4)_n \bullet HSO_4^-$. In a time-resolved analysis the clusters are seen growing from left to right by the addition of H_2SO_4 or NH_3 molecules. As the clusters grow, they take on more NH_3 molecules, depending on the experimental conditions. Higher $[NH_3]$, lower $[H_2SO_4]$ and higher temperature (T) all lead to a higher uptake of NH_3 molecules; and vice versa. Note that in any case, NH_3 molecules are found in these anion clusters only from the tetramer clusters onward (#S ≥ 4).

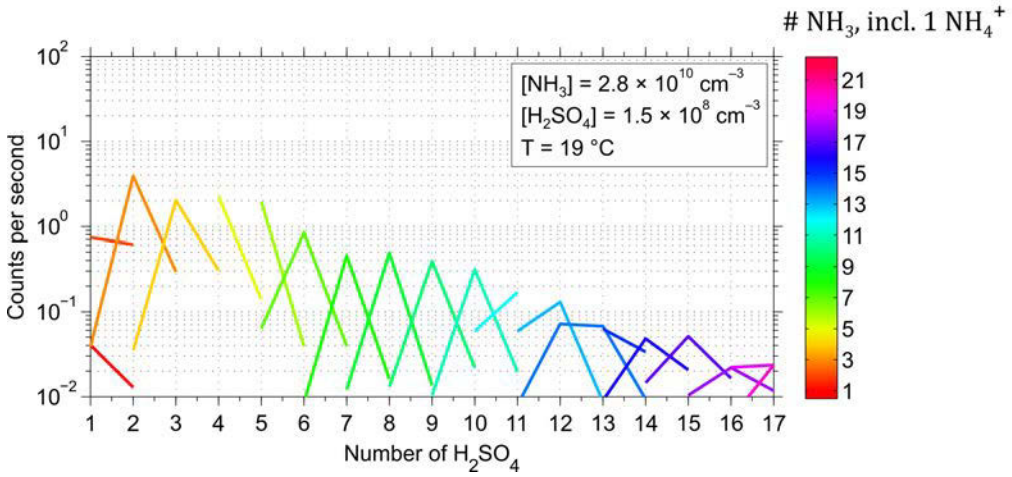

Figure 10: Results of APi-TOF measurements of positively charged ions, presented analogue to the results for negatively charged clusters in Fig. 9, for an experiment with similar conditions as in Fig. 9, top panel. Starting from the ammonium ion (NH_4^+), these clusters are $(NH_3)_m \bullet (H_2SO_4)_n \bullet NH_4^+$, with similar amounts of NH_3 molecules as in Fig. 9, top panel.

The number of NH_3 molecules in the negatively charged clusters increases with size and is further dependent on the experimental conditions. Already at only contaminant levels of $[NH_3]$, without any NH_3 added into the chamber, NH_3 is shown to be an important contributor to the formation of the negatively charged clusters (Fig. 9, center panel). These contaminant levels of $[NH_3]$ are estimated to be < 2 pptv (or $< 5 \times 10^7$ cm^{-3}). An actual binary formation mechanism, involving only H_2SO_4 and presumably H_2O, could only be achieved at high enough $[H_2SO_4]$ (Fig. 9, bottom panel), or by decreasing the temperature.

Positively charged NH_3-H_2SO_4 clusters are only observed at higher $[NH_3]$. At these high $[NH_3]$, the growth of ion clusters of both polarities proceeds by the stepwise addition of about one NH_3 molecule per H_2SO_4 molecule (Fig. 9, top panel; Fig. 10). This ratio of NH_3 to H_2SO_4 addition of close to 1:1 is consistent with the formation of ammonium bisulfate (NH_4HSO_4), the NH_3 partially neutralizing the H_2SO_4 molecules with regard to their acidity. Similar positively and negatively charged clusters with an NH_3:H_2SO_4 addition ratio of ~1:1 have also been produced and measured in other experiments, though only up to about 15 molecules, using a variety of production methods (Hanson and Eisele, 2002; Bzdek et al., 2011; Froyd and Lovejoy, 2012).

These results strongly suggest that it is acid-base chemistry rather than thermodynamics that controls the initial formation of these clusters. Note that NH_3 only binds to negatively charged sulfuric acid clusters containing at least 4 sulfur atoms. This is explained by the bisulfate ion HSO_4^- itself acting as a strong Lewis base, and as such

HSO_4^- is competing with the regular bases such as NH_3. As a result, the weaker base NH_3 can only bind to anion clusters with at least three H_2SO_4 molecules in addition to the HSO_4^- ion. In this case therefore, the enhancement of the formation of sulfuric acid clusters due to electric charge is at least in part due to essentially the same mechanism of acid-base stabilization.

The APi-TOF can only measure electrically charged clusters, and any conclusions from its results about neutral clusters can only be inferred. Model calculations that simulate the kinetics of molecules and inter-molecular forces are not bound by this limitation. Such simulations were conducted for **Paper II**, using the Atmospheric Cluster Dynamics Code (ACDC) kinetic model (McGrath et al., 2012), and evaporation rates resulting from the stability of clusters that result from ab-initio quantum chemical calculations (Ortega et al., 2012). Ions and electric charging are modeled as well, and sink terms are included according to the parameters of the experiments at CLOUD. Comparing the modeled with the measured steady-state distributions of negatively charged clusters ($(NH_3)_m \bullet (H_2SO_4)_n \bullet HSO_4^-$), the modeled clusters tend to contain in average 1 or 2 more NH_3 molecule(s). This difference is likely at least in part due to the weakest bound NH_3 molecule(s) being lost during the sampling by the APi-TOF, as indicated by the calculated evaporation rates for NH_3 or H_2SO_4 from each cluster. The very weak or absent binding of NH_3 to anion clusters with #S < 4 is reproduced well by the model; as are the general dependencies of cluster concentrations on $[NH_3]$ and $[H_2SO_4]$ (**Paper II**).

Two major limitations of the model used in **Paper II** are that the effects of water are not taken into account, and that it includes only clusters containing up to five H_2SO_4 or NH_3 molecules explicitly. Improvements regarding both limitations are likely to be implemented in the future (e.g., Paasonen et al., 2012). One very important advantage of the model, as mentioned, is the ability to obtain results for the electrically neutral case as well. In the case of high $[NH_3]$, the resulting neutral cluster distribution from #S = 1 onward is remarkably similar to the negatively charged equivalent starting from #S = 3 or 4, and it reproduces the addition ratio of NH_3 and H_2SO_4 molecules of ~1:1 (**Paper II**). Evidently, the effect of electric charge on the cluster's composition, in this case the presence of the HSO_4^- ion, is largely cancelled out once it has reached a size large enough (#S ≈ 4). HSO_4^- has then been "neutralized" by the H_2SO_4 molecules in the cluster in the sense of its basic properties.

3.2.2 Towards atmospheric particle formation rates by involving amines

The first experiments at CLOUD showed with previously unachieved clarity that NH_3, H_2O and H_2SO_4 are together not capable of explaining new particle formation in the boundary layer. However, it is in the boundary layer that most measurements are taken

and most new particle formation is observed (Kulmala et al., 2004c). Other base compounds have been suggested to be involved in boundary layer new particle formation; e.g. amines, which were found in aerosol during new particle formation events (e.g., Smith et al., 2010), in particular dimethylamine, C_2H_7N (Mäkelä et al., 2001). Quantum chemical simulations have subsequently shown that dimethylamine binds much more strongly with H_2SO_4 than NH_3 (Kurtén et al., 2008), suggesting that dimethylamine enhances new particle formation from H_2SO_4 and H_2O more effectively than NH_3. The stronger binding of dimethylamine to H_2SO_4 was demonstrated also by the experimental finding that dimethylamine at sufficiently high concentrations would even replace NH_3 molecules in already formed clusters with H_2SO_4 (Bzdek et al., 2010; 2011). Already in the very first experiments at the CLOUD chamber in 2009, not only contaminant NH_3 was found together with H_2SO_4 in growing ionic clusters, but also contaminant amines and amides, primarily C_2H_7N, which must be either ethylamine or dimethylamine. These observations of amine-H_2SO_4 clusters in a clean chamber, without deliberately adding any amines, are yet another clear indication of the strong binding between amines and H_2SO_4.

Therefore in the 4th CLOUD campaign, in the summer of 2011, a main goal was to systematically investigate the formation of particles from dimethylamine, H_2SO_4 and H_2O, at atmospherically relevant concentrations of these precursors. The contaminant level of dimethylamine in the CLOUD chamber is estimated to be < 0.1 pptv (or < 2.6×10^6 cm^{-3}). By adding only 3 pptv of dimethylamine, we found that the particle formation rates are enhanced more than 100-fold compared to the rates obtained from the NH_3-H_2O-H_2SO_4 system at [NH_3] up to 250 pptv (**Paper III**). At dimethylamine concentrations of 5 to 10 pptv, the relative enhancement saturates at a factor of about 1000. As a result, the measured particle formation rates are comparable to atmospheric observations at typical atmospheric concentrations of H_2SO_4. Results from the ACDC simulations show a similarly large enhancement of particle formation rates.

As in the earlier experiments, the results from the APi-TOF reveal the formation and growth mechanisms of the clusters during the particle formation experiments. The mechanism for the dimethylamine-H_2O-H_2SO_4 system is remarkably similar to the case of the NH_3-H_2O-H_2SO_4 system: The clusters are in general $(C_2H_7N)_m \bullet (H_2SO_4)_n \bullet HSO_y^-$ (y = 4, 5) and $(C_2H_7N)_m \bullet (H_2SO_4)_n \bullet C_2H_8N^+$, and they grow by the step-wise addition of dimethylamine and H_2SO_4 molecules at a ratio of ~1:1 (Fig. 11B; **Paper III**). This preferred base-to-acid ratio of ~1:1 was also found in independent experiments (e.g., Bzdek et al., 2011). A crucial difference between the dimethylamine case and the NH_3 case is that dimethlyamine binds already to negatively charged clusters containing three sulfur atoms, whereas NH_3 requires four (Figs. 11A, B; **Papers II–IV**). Additionally, the CIMS measurements provided evidence that the concentrations of electrically neutral sulfuric acid dimer clusters, x • $(H_2SO_4)_2$, are 5 to

6 orders of magnitude higher at the presence of 5 pptv of dimethylamine than without (**Paper III**). Such a stabilization of $x \bullet (H_2SO_4)_2$ at low and difficult to measure concentrations of x has been suggested previously based on results of flow tube measurements using a similar CIMS (Petäjä et al., 2011). The observation at CLOUD is quantitatively predicted by the ACDC simulations and very likely due to stabilization of many dimer clusters by dimethylamine, i.e., x = $(\text{dimethylamine})_m$ (Kurtén et al., 2011; **Paper III**). (Note that any dimethylamine is lost after charging of a sulfuric acid dimer cluster in the CIMS, due to the creation of an HSO_4^- ion, i.e. for the same reason that the APi-TOF does not observe any negatively charged sulfuric acid dimer cluster containing dimethylamine.)

All these observations and model results can generally be explained as being due to dimethylamine forming very strong bonds with H_2SO_4 molecules; in particular stronger bonds than NH_3 or H_2O. Note that the enhancement of particle formation rates by the inclusion of the ion-induced pathway is much smaller in the case of dimethylamine-H_2SO_4 clustering. Also this difference is qualitatively explained by dimethylamine being a stronger base than NH_3, so that the potency of the HSO_4^- ion as a Lewis base is relatively less important. Again, the chemical property of the HSO_4^- ion as a base outweighs the physical effects of its electric charge.

Note that in the CLOUD experiments, the ion could also be HSO_5^- instead of HSO_4^-; usually associated with conditions of low [H_2SO_4]. However, the composition of the growing clusters was largely unaffected. Very likely therefore, HSO_5^- has similar chemical properties as HSO_4^-.

The involvement of dimethylamine alone does not yet solve the phenomenon of boundary layer particle formation, although high particle formation rates are achieved at atmospherically relevant concentrations of H_2SO_4. Namely, it does not explain high ambient formation rates often observed also at relatively low concentrations of H_2SO_4. Also, amine concentrations, which are difficult to measure at low levels, may be well below a few pptv in the atmosphere (Ge et al., 2011; Hanson et al., 2011). Indeed, evidence of their importance in actual new particles formation in the atmosphere has been indirect and eventually remained speculative (Mäkelä et al., 2001; Smith et al., 2010; Kulmala et al., 2013). It remains to be determined where specifically particle formation occurs from amines and H_2SO_4 in the boundary layer, and how large the overall impact of such occurrences is.

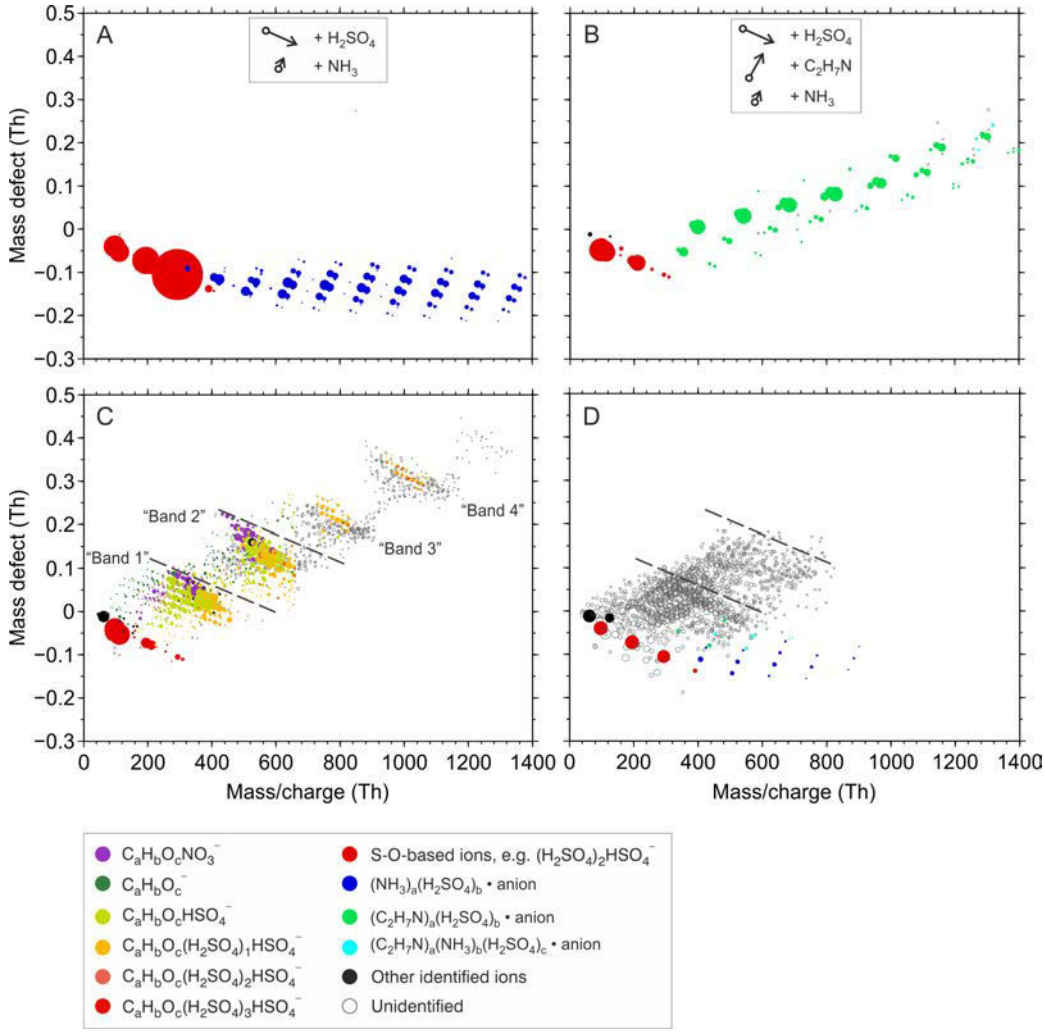

Figure 11: A summary of the APi-TOF mass spectra measured for negatively charged ions during new particle formation experiments at the CLOUD chamber (A–C), and during a new particle formation event in the boreal forest in Hyytiälä (D), adapted from **Paper IV**. The CLOUD experiments are for particle formation with H_2SO_4 and: NH_3 (A), dimethylamine, C_2H_7N (B), and oxidation products of pinanediol (C). Colors show the chemical composition, circle sizes are related to count rates. Panel A presents essentially the same data as in Fig. 9, top panel. Panels A and B show the growth of anion clusters by a stepwise addition of NH_3 and H_2SO_4 (A), and dimethlyamine and H_2SO_4, (B). For the case of oxidation products of pinanediol, the clusters grow mainly by the addition of large oxidized organics, mainly $C_{10}H_xO_y$, resulting in a distinctive band structure (C). A qualitatively similar band structure is observed for the event in the boreal forest, as well as clusters containing C_2H_7N and NH_3 (D).

So far, most atmospheric measurements have only been taken at certain places and times. Continuous atmospheric measurements like those at the SMEAR stations are important and should ideally be expanded to more locations. In particular important, but rare, are comprehensive measurements that use the techniques that we found necessary for probing into the details of physics and chemistry of atmospheric particle formation, such as high-resolution mass spectrometers and CPCs with low cut-off sizes. However, comprehensive measurements using state-of-the-art techniques have already been done in the boreal forest, and they hint at a crucial role of oxidized organic compounds (Kulmala et al., 2013; **Paper IV**).

3.2.3 Towards atmospheric particle formation mechanisms by involving oxidized organics

Oxidized organic compounds are another class of compounds that has been suggested to be involved in atmospheric particle formation. It is a very broad class of compounds of the general structure $C_xH_yO_z$. Numerous such compounds have been identified in secondary organic aerosols (e.g., Hallquist et al., 2009). It is quite certain that oxidized organics participate in particle growth, already from at least 3 or 4 nm onward. Some research suggests that they can also be involved in the actual formation of particles, which happens below those sizes (Zhang et al., 2004; Metzger et al., 2010; Paasonen et al., 2010); but it has remained unclear exactly how they are involved, and from which size the involvement of organics begins (Riipinen et al., 2012). Experiments could show evidence that single organic acid molecules can combine with H_2SO_4 to form initial clusters (Zhang et al., 2009; Wang et al., 2010). But these experiments were conducted at precursor concentrations several orders of magnitude higher than typical for the atmosphere, and the initial growth was concluded to be dominated by the addition of H_2SO_4; a result likely due to the very high [H_2SO_4] in those experiments. More recent studies suggest that organics are in fact capable of condensing already at sizes below 3 nm (Donahue et al., 2011b). Indeed, there is also recent experimental evidence for organics contributing to an accelerating particle growth already from 1.5 nm onward (Kuang et al., 2012; Riccobono et al., 2012; Kulmala et al., 2013). So far however, the composition of clusters and smallest particles could not directly be measured, and the exact mechanisms of their formation have remained to be resolved.

During the 4th CLOUD campaign, we performed systematic experiments to investigate new particle formation from H_2SO_4 and oxidized organics. Monoterpenes are recognized as an important source of condensable organic species that may contribute to atmospheric new particle formation (Donahue et al., 2012a; Ehn et al., 2012). We chose to feed pinanediol ($C_{10}H_{18}O_2$) into the CLOUD chamber as a surrogate 1st oxidiation product of monoterpenes. This let us focus on one branch of α-pinene

oxidation, serving as a model compound for the wide range of monoterpenes and their oxidiation products. The practical advantage of using pinanediol is that it does not have any double bonds. Therefore it is not attacked by ozone, and we can control its oxidation by varying UV illumination in the CLOUD chamber.

As was the case for the experiments with amines, the measured particle formation rates for the oxidized organics-H_2SO_4 system are comparable to ambient observations at gas-phase concentrations of H_2SO_4 typical for the atmosphere.

The resulting mass spectra are considerably more complex during particle formation from the oxidized organics-H_2SO_4 system than in the earlier CLOUD experiments. It has proven useful to plot the mass spectra as so-called mass defect diagrams (Fig. 11; **Paper IV**). In these diagrams, the mass defect of ions (the difference between the exact mass in unified atomic mass units and the sum of all protons and neutrons) is plotted against their exact mass. Peaks in the mass spectrum are shown as circles, their size scaled by the respective count rates (= the area under the peak in the spectrum). Each elemental composition has a unique position on such a plot, and the addition of a certain molecule to an ion or ionic cluster takes the shape of a displacement on the plot by a unique vector. For the earlier experiments, the resulting diagrams are grid-like, revealing the stepwise addition of base and acid molecules (Figs. 11A, B; **Papers III–IV**). For the system of oxidized organics and H_2SO_4, the data arrange in at least four broad bands, about 220 Th apart from each other (Fig. 11C). The transition to each band represents the addition of one large oxidized organic molecule, containing mainly 10 carbon atoms. Each band consists mainly of signal from these oxidized organics, together with HSO_4^- and up to three additional H_2SO_4 molecules, i.e. $(C_{10}H_xO_y)_n \bullet (H_2SO_4)_{0–3} \bullet HSO_4^-$ with n corresponding to the band number. The span of each band from the upper left to the lower right is due to the different numbers of involved oxygen atoms and H_2SO_4 molecules, because oxygen (O) and sulfur (S) both have a large negative mass defect. Therefore, it is a wide range of oxidized organics that forms these growing clusters together with H_2SO_4 molecules. The average number of H_2SO_4 molecules in the clusters increases as the clusters grow (Fig. 11C; Fig. 12).

Some of the C_{10}-organics are surprisingly highly oxidized. The level of oxidation can be characterized by the average oxidation state of carbon, $\overline{OS_C} = 2\ n_O{:}n_C - n_H{:}n_C$ (Kroll et al., 2011). The C_{10}-organics range from $\overline{OS_C} = -1.4$ (oxygen-to-carbon ratio ≈ 0.1) to $\overline{OS_C} = 1$ (oxygen-to-carbon ratio ≈ 1.2). We also observe clusters of oxidized organics with contaminant nitrate ions, i.e. $(C_{10}H_xO_y)_n \bullet NO_3^-$, preferentially for the relatively highly oxidized organics ($\overline{OS_C} \geq -0.6$). The observation of such $(C_{10}H_xO_y)_n \bullet NO_3^-$ agrees with observations of highly oxidized organics ($0 \leq \overline{OS_C} \leq 1.2$) after the oxidation of α-pinene using a chemical-ionization APi-TOF that ionizes the sample using NO_3^- ions (Ehn et al., 2012).

The average $\overline{OS_C}$ decreases from –0.3 to –0.8 as the clusters grow from containing 10 C to containing 40 C. The high initial $\overline{OS_C}$ attests the high stability of the bond between highly oxidized organics and HSO_4^-. But the larger the clusters grow, the easier it is for more abundant but less highly oxidized organics to bind to the clusters (Fig. 12, bottom panel). Both these observations, the low volatility of highly oxidized organics and the higher abundance of less highly oxidized organics, are consistent with a model of pinanediol oxidation by OH radicals, using the 2D volatility basis set (2D-VBS) framework (Donahue et al., 2011a; 2012b; 2012a; **Paper IV**). The average $\overline{OS_C}$ of organics containing 10 C first binding to HSO_4^- broadly corresponds to 2nd C_{10}-oxidation products from pinanediol, whereas the average $\overline{OS_C}$ of organics containing 40 C corresponds to 1st C_{10}-oxidation products from pinanediol (Fig. 13). However, the detailed mechanisms behind this extensive oxidation remain to be determined.

It seems likely that these oxidized organic compounds are (poly-)acids, with additional functional groups (Donahue et al., 2013). Quantum chemical calculations using similar compounds show that they can also form stable electrically neutral clusters with H_2SO_4 instead of HSO_4^-, so the ionic clusters observed by the APi-TOF are likely similar to the neutral clusters. This hypothesis is supported by comparisons of growth rates obtained from the APi-TOF with those obtained from CPCs that measure also neutral clusters, which agree well (**Paper IV**).

When comparing the APi-TOF spectra from CLOUD with the APi-TOF spectrum measured during a new particle formation event in the boreal forest, we see a mix of the main features from all CLOUD experiments (Fig. 11D). There are clusters of H_2SO_4 with NH_3, dimethylamine, or both (though mainly with NH_3). But most of the ion signal lies in two bands at very similar positions as those of the first two bands in the CLOUD experiment with oxidized organics and H_2SO_4 (Fig. 11C). It is difficult to identify the compositions for these ions in the boreal forest case, due to the much wider range of organics involved and a lower signal-to-noise ratio. However, the few strongest peaks were identified as similar highly oxidized organic compounds (Ehn et al., 2010; 2012). They include many C_{10}-organics that were also found during oxidized organics-H_2SO_4 particle formation in the CLOUD chamber (**Paper IV**).

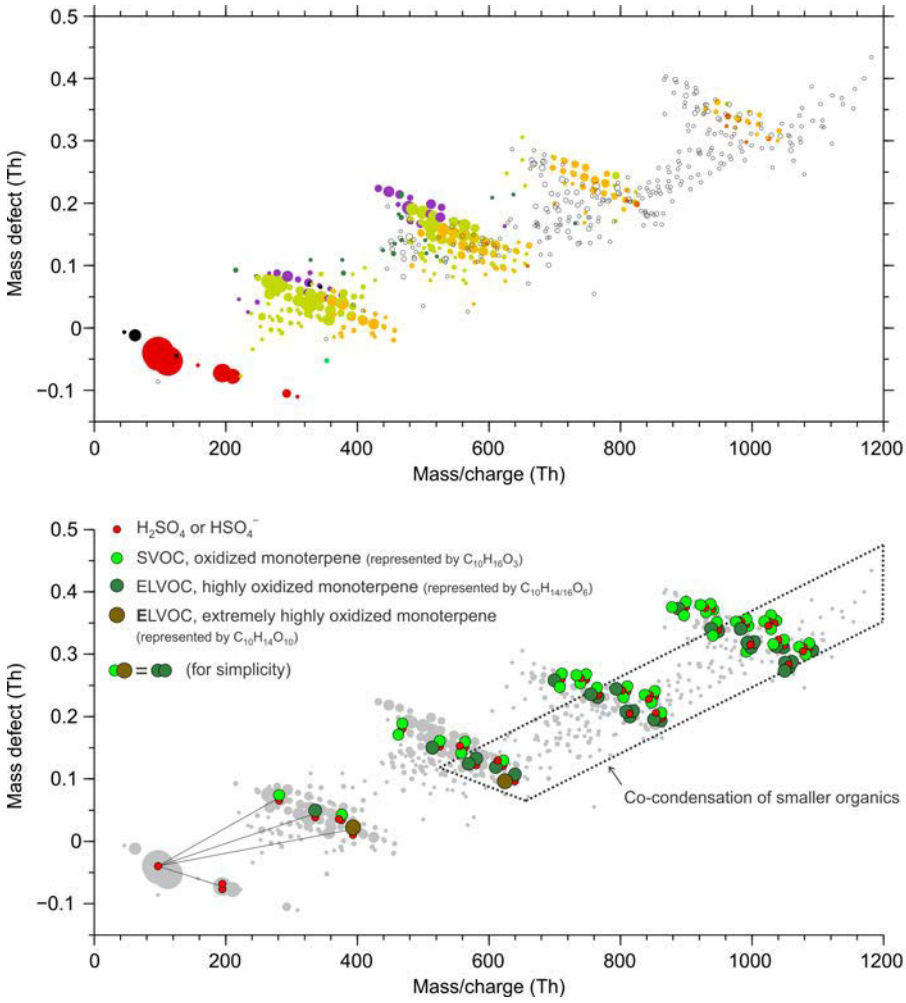

Figure 12: A more detailed and descriptive view of the ion mass spectra measured during particle formation from H_2SO_4 and organics oxidized from pinanediol in the CLOUD chamber. The top panel is a mass defect diagram for a similar experiment as in Fig. 11C, using the same color-coding as for Fig. 11. Increasing numbers of oxygen atoms cause the discrete steps of identified compounds from the upper left to the lower right within each of the four bands. The average number of H_2SO_4 molecules in the clusters increases as the clusters grow (colors from yellow to red). The bottom panel is a simplified presentation of the observed clustering. The position of each cluster is close to its actual position in the mass defect diagram. Included is a crude presentation of the different levels of oxidation involved, showing three examples of differently highly oxidized compounds. A higher oxidation state corresponds to a lower volatility, in accordance with the 2D-VBS, covering the range from semi-volatile organic compounds (SVOC) to extremely low volatility organic compounds (ELVOC). ELVOC include compounds with a wide range of oxidation states, which are here further divided into "ELVOC", representing highly oxidized compounds (e.g., $C_{10}H_{14}O_6$), and "**E**LVOC" (with a bold E), representing extremely highly oxidized compounds (e.g., $C_{10}H_{14}O_{10}$).

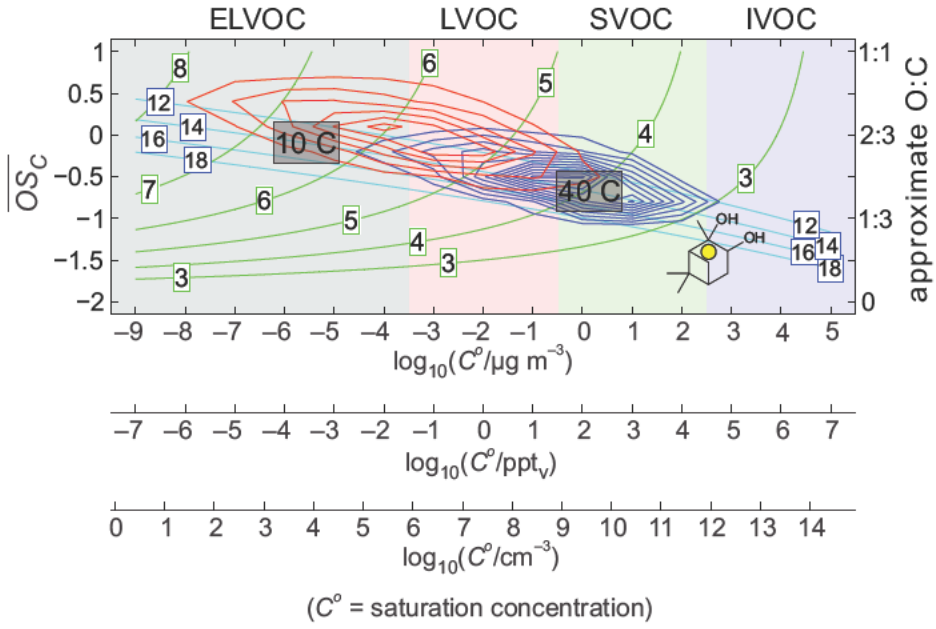

Figure 13: Representation of the oxidation of pinanediol (PD) by OH in the 2D volatility basis set using generic OH oxidation kernel; adapted from **Paper IV**. Organics are classified as intermediate volatility organic compounds (IVOC), semi-volatile organic compounds (SVOC), low volatility organic compounds (LVOC), and extremely low volatility organic compounds (ELVOC). The position of PD is represented by a yellow dot and its structure. Isolines are exclusively for C_{10}-compounds! Green lines show oxygen numbers (O); light blue lines show hydrogen numbers (H). Blue contours show functionalization products of PD oxidation (first-generation); red contours show functionalization products for second-generation products formed from a distribution of first-generation products weighted by the blue contours. Grey boxes marked "10 C" and "40 C" show the position of C_{10}-organics corresponding to the average $\overline{OS_C}$ measured for clusters containing 10 C and 40 C, respectively.

A closer look at the mass spectrum for oxidized organics-H_2SO_4 particle formation (Fig. 12) shows smaller compounds co-condensing onto ion clusters from the second band (mostly $C_{20}H_xO_y \bullet (H_2SO_4)_{0-1} \bullet HSO_4^-$) onwards. These are almost certainly smaller organics (#C < 10). This observation may be interpreted as stable clusters constituting a large enough seed to allow for the condensation of vapors that would otherwise not condense. However, the main contributors to the growth to at least 1.6–1.7 nm (the 4th band) are C_{10}-organics, at least for conditions as in Fig. 11C and Fig. 12.

As a summary, the combined picture of the results from the controlled experiments at CLOUD and their comparison to ambient observations in the boreal forest suggests that large oxidized organic compounds are crucial in atmospheric particle formation, at least

in the boreal forest. NH_3 and dimethylamine probably only play a supporting role; because NH_3 alone is found not to sufficiently stabilize small H_2SO_4 clusters (section 3.2.1) and dimethylamine concentrations are apparently so low that they do not even replace NH_3 as the dominant small base in the clusters with H_2SO_4 (Fig. 11D). Indeed, more recent measurements of particle formation in the boreal forest found evidence that an initial increase of $[H_2SO_4]$ leads to only small, slowly growing, but stable clusters, whereas the additional availability of large oxidized organics initiates a faster growth of these clusters into particles larger than 2 nm (Kulmala et al., 2013). For the CLOUD experiments with pinanediol, the corresponding stable clusters may be $C_{20}H_xO_y \bullet (H_2SO_4)_{0-1} \bullet HSO_4^-$, which allow for the subsequent growth to be aided by the smaller organics that are present in the mix of organics in the CLOUD chamber.

The results from all the experiments at CLOUD also suggest that it will eventually depend on the prevailing conditions, which compounds will play an active role in new particle formation in the atmosphere. In particular, the concentrations of vapors able to participate in particle formation are probably crucial, as well as physical parameters (such as temperature) and meteorological conditions (mixing). In these terms, conditions can vary significantly, both horizontally and vertically.

3.3 Measuring new particle formation from above the canopy to the free troposphere

New particle formation has been observed throughout the troposphere: at the ground, in the boundary layer, as well as in the free troposphere. Most of the measurements of new particle formation events so far have been made at the ground (e.g., Kulmala and Kerminen, 2008). The horizontal extent of these events can usually be inferred from these ground-based measurements, because for most events, both the formation and the subsequent growth can be observed at a single site, often for many continuous hours (Kulmala et al., 2001b; Dal Maso et al., 2005). Such observations can only be explained by a regional scale of these events (e.g., Mäkelä et al., 1997; Charron et al., 2007). Networks of measurement stations can provide information on the horizontal scale of events as well (Wehner et al., 2007; Komppula et al., 2006). The horizontal extent of regional scale events was found to be of the order of 500 km (Hussein et al., 2009).

Airborne measurements confirmed the regional scales of many new particle formation events. Some also managed to define horizontal boundaries of these events: E.g., O'Dowd et al. (2009) found that the new particle formation event did not extend into the air over the frozen sea. In addition, airborne measurements provide information on the vertical extents of new particle formation (e.g., Crumeyrolle et al., 2010; Hamburger et al., 2011; Mirme et al., 2010). Airborne measurements over the Finnish boreal forest were conducted already in 2003 during few new particle formation events

using a DHC-6 Twin Otter airplane (O'Dowd et al., 2007, 2009). These and other airborne measurements confirmed that regional-scale events extend throughout the boundary layer, but not into the free troposphere above. Questions that remain are: Where exactly in the boundary layer does the new particle formation start, or is it evenly distributed; and what is the role of boundary layer dynamics, both in terms of mixing within it and in terms of interactions with other layers, such as the residual layer and the free troposphere. So far, our knowledge of new particle formation above the ground (or above the reach of towers and masts) is limited to indirect, ground-based measurements, and to only few direct airborne measurements. The main reason for the rarity of airborne measurements may be that they tend to be expensive. In addition, they generally entail extra complications: E.g., aviation regulations need to be conformed to, power supply for instruments can be a problem, or sampling from a moving (often fast-moving) aircraft may require special considerations.

In Spring 2009, the first measurement flights took place, commissioning a Cessna 172 as a relatively simple and inexpensive platform for airborne aerosol measurements. Experimental details are provided in section 2.3.1, as well as in **Paper V**. The main advantages of this platform are low operating costs compared to larger airborne measurement setups, and that it is simpler to conform to the regulations. Another feature is the airplane's relatively low speed, which translates to a relatively high spatial resolution of the measurements. One goal of the first flights was to verify the quality and usability of the recorded data, to identify problems as well as possibilities for improving the setup. In this respect, we found one model of CPCs (TSI 3772) not suitable for measurements on the Cessna, because it often produced erroneous results at higher altitudes (> 2 km). The problem is probably related to low pressure, tilting of the instrument, and maybe vibrations. The other CPCs used (TSI 3776 and TSI 3010) worked without any complications. We also found that a more complete aerosol size distribution would be desirable, as well as a camera for taking record of prevailing conditions. During 2010 therefore, the two TSI 3772 CPCs were replaced by an SMPS, and a web camera was installed. Both upgrades were successfully tested.

The scientific goal was to explore the horizontal and vertical extent of several new particle formation events, ideally at their different stages, in particular at the start of particle formation. This goal was achieved for at least two new particle formation events in 2009 (**Paper V**). The covered heights range from about 50 m to about 3500 m above ground, i.e., from close to the forest canopy to the free troposphere. We confirmed earlier measurements in that the new particle formation events extended vertically throughout the boundary layer and horizontally over all land overflown, which was up to about 100 km from the SMEAR II station. Inhomogeneities in particle concentrations were generally observed horizontally and vertically, probably due to geographical variations. In average however, larger concentrations were found in the

upper parts of the boundary layer. This observation supports previous direct ground-based (Venzac et al., 2008) and airborne measurements (Crumeyrolle et al., 2010) that similarly reported on the importance of new particle formation in the upper boundary layer. Additionally, we found that the concentrations of 3–6 nm particles, the smallest particles measured, were generally higher throughout the boundary layer than the corresponding concentrations measured at the SMEAR II station. These results suggest that dynamics in the upper boundary layer are indeed inducive of particle formation, e.g., entrainment fluxes at the top of the boundary layer. This suggestion has been made also previously, based mainly on indirect ground-based measurements (Nilsson et al., 2001; Pryor et al., 2011; Crippa et al., 2012). Local enhancements of new particle formation could also be observed due to local reductions of condensation and coagulation sinks that may have been the result of cloud processing. In one instance, evidence for local new particle formation was found in a layer just above clouds, i.e. possibly in its outflow. Note that the onboard instrumentation at the time could not address atmospheric dynamics. This drawback has since been remedied by the installation of a turbulence probe for future measurements.

4 Review of papers and author's contributions

Paper I reports on experimental investigations of the temperature dependence of heterogeneous nucleation of n-propanol on silver and NaCl seed particles of sizes from 4 to 11 nm. A well-controlled laboratory setup was used that initiates the heterogeneous nucleation of vapor on seed particles by rapid adiabatic expansion. The shrinkage of NaCl particles due to the presence of n-propanol was also measured, as well as the temperature dependence of the contact angle of n-propanol on NaCl particles. The main result was a reversed temperature dependence compared to the dependence anticipated from classical theory for the nucleation onto NaCl particles. Such reversal was not observed for silver particles. The results suggest an important role of inter-molecular forces that are not taken into account by classical theories. I conducted all measurements and analysis of the resulting data, with the exception of the contact angle measurements. In addition, I adapted existing Fortran codes to perform the theoretical calculations, and did almost all the writing.

Paper II presents results of simulations of electrically charged and neutral ammonia-sulfuric acid clusters using a dynamic collision and evaporation model. Evaporation rates resulted from first-principle quantum chemical calculations with no fitted parameters. The simulation results were compared with the corresponding results of the direct measurements of the APi-TOF mass spectrometer of charged ammonia-sulfuric acid clusters during particle formation experiments at the CLOUD chamber. The

agreement was good, and information on neutral clusters was gained that cannot yet be measured. I was responsible for the APi-TOF measurements and its setup at the CLOUD chamber, participated in the corresponding measurement campaigns, and did all of the APi-TOF data analysis. I wrote the parts of the paper explaining the APi-TOF measurements and data analysis, and the experimental part of the discussion of sources of uncertainties and errors, and participated in the interpretation of the results.

Paper III presents the results of the measurements of new particle formation from dimethylamine and sulfuric acid that were conducted at the CLOUD chamber. It was found that very small amounts of dimethylamine are able to substantially enhance the formation of particles from sulfuric acid, resulting in significant formation rates at atmospherically relevant conditions. The APi-TOF measurements reveal the mechanism by which this formation proceeds, supported by the results of chemical ionization mass spectrometers. The enhancement of particle formation rates is found to be due to a very strong binding of dimethylamine to sulfuric acid, and the results are well reproduced by quantum chemical calculations of the binding energies in dimethylamine-sulfuric acid clusters. I was responsible for the APi-TOF measurements and its setup at the CLOUD chamber, and participated in the corresponding measurement campaigns. I did all of the APi-TOF data analysis and prepared the corresponding figures in the paper. I participated in the interpretation of the results and commented on the manuscript.

Paper IV presents comprehensive results of APi-TOF measurements, mainly from measurements at the CLOUD chamber, with the focus on new particle formation experiments from sulfuric acid and oxidation products of pinanediol. The observations showed that large oxidized organics clustered directly with single sulfuric acid molecules and then formed growing clusters of one to three sulfuric acid molecules and up to four oxidized organics. The organics are products of the oxidation of monoterpenes, and some were remarkably highly oxidized. The average degree of oxygenation decreased as the clusters grew. A remarkable resemblance was revealed between the mass spectra from these experiments and corresponding mass spectra recorded during new particle formation in the boreal forest, concluding that similar clusters between oxidized organics and sulfuric acid are crucial for new particle formation in the atmosphere. I was responsible for the APi-TOF measurements and its setup at the CLOUD chamber, participated in the corresponding measurement campaigns, and did all of the APi-TOF data analysis. I wrote most of the main text and all of the supporting information.

Paper V presents the new airborne measurement setup used with the Cessna 172 aircraft, as well as the results from the first measurement flights conducted during new particle formation event days in 2009 and 2010. The measurement platform proved to

work well, and was improved according to gathered experience. A comprehensive description of results is provided for selected flights. The main results were the observation of new particle formation events throughout the boundary layer, in line with previous observations, and indications for dynamic processes playing a role in these events. I participated in preparing the airborne measurements and conducted several measurement flights during 2009. I analyzed most of the data and wrote most of the paper.

5 Conclusions

Many critical processes in the field of aerosol science include phase transitions and can be described by classical nucleation theory, which has been developed from macroscopic principles of thermodynamics. As one objective of this thesis, we specifically tested the applicability of classical heterogeneous nucleation theory to the nucleation of vapor onto 4–11 nm seed particles of different materials (**Paper I**). We found that classical nucleation theory can fail at these small sizes, probably because inter-molecular forces start to play an important role. These interactions are material-specific and cannot be practically described by the classical theories. Indeed, batteries of CPCs with different working fluids have successfully exploited such material-specific effects. They have used the different nucleation properties of different working fluids on a certain material, in order to investigate the chemical properties of sub-10 nm aerosol (Kulmala et al., 2007; Riipinen et al., 2009). Note that later experiments that employed suitable mass spectrometric techniques, such as the APi-TOF (e.g., **Papers II–IV**), demonstrated that contaminant levels of impurities can have an important impact on the actual composition of at least sub-2 nm aerosol. However, the seed particles in **Paper I** are probably sufficiently pure NaCl or Ag, mainly because of their larger size ($\geq$ 4 nm) and their production in large quantities in a tube furnace.

The critical initial processes that lead to atmospheric new particle formation take place at very small sizes, namely below 2 nm (Kulmala et al., 2013). Novel experimental and theoretical techniques have been developed to directly access this size regime, particularly in the last five years. The most important of these experimental techniques are diethylene glycol-based CPCs, such as the PSM, and APi-TOF mass spectrometers. Theoretical techniques include the ACDC model and quantum-chemical ab-initio studies. As the main work here, those new experimental techniques were employed to investigate atmospheric new particle formation, in particular the APi-TOF, and mainly during particle formation experiments in the CLOUD chamber.

As shown in this thesis, the APi-TOF measurements were extremely successful in particular in combination with the CLOUD experiment (**Papers II–IV**). A good

summary of the results of these measurements is given by Fig. 11. The investigated systems of vapors were: ammonia + sulfuric acid (Fig. 11A), dimethylamine + sulfuric acid (Fig. 11B), and oxidation products from pinanediol + sulfuric acid (Fig. 11C). For each system, the APi-TOF could directly measure the composition of ions and the formation and growth mechanisms of ionic clusters that lead to the formation of particles. The APi-TOF results also revealed that even tiny concentrations of impurities in the experiment can be critical and be involved in these processes. Consequently, as low as possible concentrations of contaminants turned out to be crucial when one wants to systematically investigate the processes that are relevant to atmospheric new particle formation. Indeed the CLOUD facility's ability to provide unprecedented levels of cleanliness turned out to be a key to the success of the APi-TOF measurements in particular, and the CLOUD experiments in general.

The direct measurements of ionic clusters by the APi-TOF further presented the possibility of directly comparing these experimental observations with state-of-the-art cluster simulations. For **Paper II**, the formation of ammonia-sulfuric acid clusters in the CLOUD chamber was simulated using the ACDC model, which uses kinetic collisions and evaporation rates based on quantum chemical calculations. The simulations achieved a good agreement with the measurement results. They confirmed that the APi-TOF measurements were subject to only little fragmentation of clusters during the sample process. Additionally, the simulations could directly investigate also the electrically neutral pathway of cluster formation, which cannot be directly accessed by the APi-TOF measurements.

The APi-TOF measurements have substantially contributed in improving our detailed understanding of atmospheric new particle formation. Together with model simulations and the entirety of measurements taken during the CLOUD experiments (e.g., CPC measurements of particle formation rates), they offered unprecedented insight on the initial steps of particle formation (Kirkby et al., 2011; **Papers II–IV**).

A main finding was that inter-molecular chemistry dominates the mechanism, by which the initial clusters form. At least in the case of ammonia + sulfuric acid and dimethylamine + sulfuric acid, the mechanism is acid-base chemistry in the form of strong hydrogen bonds. Dimethylamine molecules form stronger bonds with sulfuric acid molecules (H_2SO_4) than ammonia, which is the reason for getting substantially higher particle formation rates from dimethylamine + sulfuric acid than from ammonia + sulfuric acid (**Paper III**). For anions, the enhancement of the formation of clusters and particles is in fact due to the very same acid-based chemistry, rather than due to electrostatic attraction. Much of the negative charge comes in the form of HSO_4^- bisulfate ions (and HSO_5^- ions), which is a strong Lewis base (as is HSO_5^-, though less strong). They compete against ammonia and dimethylamine for binding with H_2SO_4, although more successfully against ammonia, because it is a weaker base than

dimethylamine. As a result, the charge enhancement on formation rates is stronger for the case of ammonia + sulfuric acid than for the case of dimethylamine + sulfuric acid.

In the CLOUD experiments, atmospherically relevant particle formation rates were also measured with H_2SO_4 and oxidized organics that were obtained from the oxidation of pinanediol, a surrogate 1st oxidation product of monoterpenes. Again, the APi-TOF measurements revealed details of the underlying mechanisms (**Paper IV**). We found that these oxidized organics can directly form clusters with HSO_4^- and with $H_2SO_4 \bullet HSO_4^-$; and very likely also with H_2SO_4 and with $(H_2SO_4)_2$. Predominantly it is large oxidized organics that form these clusters, mostly with 10 carbon atoms, and some of them highly oxidized. They correspond to 2nd and 3rd oxidation products of monoterpenes. The clusters grow by subsequent addition of more of these large oxidized organics and H_2SO_4, and their oxidations state decreases as they grow. We further found indications that certain clusters of two or more large oxidized organics together with one or more H_2SO_4 can facilitate the co-condensation of smaller organics. Importantly, comparisons with measurements at the SMEAR II station (cf. Fig. 11C and Fig. 11D) suggest that similar large oxidized organics play a key role in new particle formation in the boreal forest.

As part of this thesis, we also performed airborne measurements to map out regional-scale particles formation events both vertically and horizontally. For this purpose, an airborne measurement platform was commissioned and successfully tested (**Paper V**). The results mainly complemented previous observations. The whole boundary layer was confirmed as the location of regional-scale particle formation events, and locally confined instances or enhancements of new particle formation were observed and associated with dynamic processes related to clouds. These were the results from only the first measurement flights in 2009 and 2010. Since then, more flights have been conducted. Improvements on the measurement setups are being implemented continuously, also as a result of the experience gathered during the flight measurements in 2009 and 2010.

The main objective of this thesis was to advance our knowledge of the physical and chemical mechanisms behind the formation of new particles in the atmosphere. A great increase of our detailed understanding of this process was attained mainly by the application of recently developed state-of-the-art experimental techniques. They were applied both in well-controlled laboratory setups and in the field. In particular, mass spectrometers have proven to be a critical new tool in accessing molecular clusters in the sub-2 nm regime during particle formation studies. Advances in computational techniques have also proven important, as they allow for simulating processes critical for new particle formation – both those processes that are now experimentally accessible, and those yet inaccessible. In addition, this work demonstrated the importance of taking particle formation measurements afield and aloft.

References

Aalto P. P., Hämeri K., Becker E., Weber R., Salm J., Mäkelä J. M., Hoell C., O'Dowd C. D., Karlsson H., Hansson H.-C., Väkevä M., Koponen I. K., Buzorius G., Kulmala M.: Physical characterization of aerosol particles during nucleation events, *Tellus*, 53B, 344-358 (2001).

Abraham F. F.: Multistate kinetics in nonsteady-state nucleation: A numerical solution, *J. Chem. Phys.*, 51, 1632-1638 (1969).

Aitken J.: On improvements in the apparatus for counting the dust particles in the atmosphere, *Proc. Roy. Soc. Edinburgh*, 16, 207-235 (1889).

Andreae M. O., Rosenfeld D.: Aerosol–cloud–precipitation interactions. Part 1. The nature and sources of cloud-active aerosols, *Earth-Sci. Rev.*, 89, 13-41 (2008).

Ångström A.: On the atmospheric transmission of sun radiation and on dust in the air, *Geogr. Ann.*, 11, 156-166 (1929).

Apte J. S., Kirchstetter T. W., Reich A. H., Deshpande S. J., Kaushik G., Chel A., Marshall J. D., Nazaroff W. W.: Concentrations of fine, ultrafine, and black carbon particles in auto-rickshaws in New Delhi, India, *Atmos. Env.*, 45, 4470-4480 (2011).

Bae M.-S., Schwab J. J., Hogrefe O., Frank B. P., Lala G. G., Demerjian K. L.: Characteristics of size distributions at urban and rural locations in New York, *Atmos. Chem. Phys.*, 10, 4521-4535 (2010).

Benson D. R., Li-Hao Y., Shan-Hu L., Campos T. L., Rogers D. C., Jensen J.: The effects of airmass history on new particle formation in the free troposphere: case studies, *Atmos. Chem. Phys.*, 8, 3015-3024 (2008).

Bianchi F., Dommen J., Mathot S., Baltensperger U.: On-line determination of ammonia at low pptv mixing ratios in the CLOUD chamber, *Atmos. Meas. Tech.*, 5, 1719-1725 (2012).

Biskos G., Malinowski A., Russell L. M., Buseck P. R., Martin S. T.: Nanosize effect on the deliquescence and the efflorescence of sodium chloride particles, *Aerosol Sci. Tech.*, 40, 97-106 (2006).

Bzdek B. R., Ridge D. P., Johnston M. V.: Size-dependent reactions of ammonium bisulfate clusters with dimethylamine, *J. Phys. Chem. A*, 114, 11638-11644 (2010).

Bzdek B. R., Ridge D. P., Johnston M. V.: Amine reactivity with charged sulfuric acid clusters, *Atmos. Chem. Phys.*, 11, 8735–8743 (2011).

Carslaw K. S., Lee L. A., Reddington C. L., Mann G. W., Pringle K. J.: The magnitude and sources of uncertainty in global aerosol, *Farad. Discuss.*, 165, 495-512 (2013).

Charlson R. J., Schwartz S. E., Hales J. M., Cess R. D., Coakley J. A., Hansen J. E., Hofmann D. J.: Climate forcing by anthropogenic aerosols, *Science*, 255, 423-430 (1992).

Charron A., Birmili W., Harrison R. M.: Factors influencing new particle formation at the rural site, Harwell, United Kingdom, *J. Geophys. Res.*, 112, D14210 (2007).

Clarke A. D.: Atmospheric nuclei in Pacific midtroposphere: Their nature, concentration and evolution, *J. Geophys. Res.*, 98, 20633 - 20647 (1993).

Clarke A. D., Kapustin V.: Hemispheric aerosol vertical profiles: Anthropogenic impacts on optical depth and cloud nuclei, *Science*, 329, 1488 (2010).

Coakley J. A., Bernstein R. L., Durkee P. A.: Effect of ship-stack effluents on cloud reflectivity, *Science*, 237, 1020-1022 (1987).

Coffman D. J., Hegg D. A.: A preliminary study of the effect of ammonia on particle nucleation in the marine boundary layer, *J. Geophys. Res.*, 100, 7147-7160 (1995).

Craig A., McIntosh R.: The preparation of sodium chloride of large specific surface, *Can. J. Chem.*, 30, 448-453 (1952).

Crippa P., Petäjä T., Korhonen H., El Afandi G. S., Pryor S. C.: Evidence of an elevated source of nucleation based on model simulations and data from the NIFTy experiment, *Atmos. Chem. Phys.*, 12, 8021-8036 (2012).

Crumeyrolle S., Manninen H. E., Sellegri K., Roberts G., Gomes L., Kulmala M., Weigel R., Laj P., Schwarzenboeck A.: New particle formation events measured on board the ATR-42 aircraft during the EUCAARI campaign, *Atmos. Chem. Phys.*, 10, 6721-6735 (2010).

Curtius J., Lovejoy E. R., Froyd K. D.: Atmospheric Ion-Induced Aerosol Nucleation. In: *Solar Variability and Planetary Climates*, [Calisesi Y., Bonnet R. M., Gray L., Langen J., Lockwood M. (Eds.)], Space Sciences Series of ISSI, Springer, New York (2007).

Dal Maso M., Kulmala M., Lehtinen K. E. J., Mäkelä J. M., Aalto P., O'Dowd C. D.: Condensation and coagulation sinks and formation of nucleation mode particles in coastal and boreal forest boundary layers, *J. Geophys. Res.*, 107, PAR 2-1-PAR 2-10 (2002).

Dal Maso M., Kulmala M., Riipinen I., Wagner R., Hussein T., Aalto P. P., Lehtinen K. E. J.: Formation and growth of fresh atmospheric aerosols: eight years of aerosol size distribution data from SMEAR II, Hyytiälä, Finland, *Boreal Env. Res.*, 10, 323-336 (2005).

de Hoffmann E., Stroobant V.: *Mass Spectrometry: Principles and Applications - 3rd ed.*, John Wiley & Sons, Chichester, England (2007).

Donahue N. M., Epstein S. A., Pandis S. N., Robinson A. L.: A two-dimensional volatility basis set: 1. organic-aerosol mixing thermodynamics, *Atmos. Chem. Phys.*, 11, 3303-3318 (2011a).

Donahue N. M., Trump E. R., Pierce J. R., Riipinen I.: Theoretical constraints on pure vapor-pressure driven condensation of organics to ultrafine particles, *Geophys. Res. Lett.*, 38, L16801 (2011b).

Donahue N. M., Henry K. M., Mentel T. F., Kiendler-Scharr A., Spindler C., Bohn B., Brauers T., Dorn H. P., Fuchs H., Tillmann R., Wahner A., Saathoff H., Naumann K.-H., Möhler O., Leisner T., Müller L., Reinnig M.-C., Hoffmann T., Salo K., Hallquist M., Frosch M., Bilde M., Tritscher T., Barmet P., Praplan A. P., DeCarlo P. F., Dommen J., Prévôt A. S. H., Baltensperger U.: Aging of biogenic secondary organic aerosol via gas-phase OH radical reactions, *Proc. Natl. Acad. Sci. USA*, 409, 13503–13508 (2012a).

Donahue N. M., Kroll J. H., Pandis S. N., Robinson A. L.: A two-dimensional volatility basis set – Part 2: Diagnostics of organic-aerosol evolution, *Atmos. Chem. Phys.*, 12, 615-634 (2012b).

Donahue N. M., Chuang W., Ortega I. K., Riipinen I., Riccobono F., Schobesberger S., Dommen J., Kulmala M., Worsnop D. R., Vehkamäki H.: How do organic vapors contribute to new-particle formation?, *Farad. Discuss.*, 165, 91-104 (2013).

Duplissy J., Enghoff M. B., Aplin K. L., Arnold F., Aufmhoff H., Avngaard M., Baltensperger U., Bondo T., Bingham R., Carslaw K., Curtius J., David A., Fastrup B., Gagné S., Hahn F., Harrison R. G., Kellett B., Kirkby J., Kulmala M., Laakso L., Laaksonen A., Lillestol E., Lockwood M., Mäkelä J., Makhmutov V., Marsh N. D., Nieminen T., Onnela A., Pedersen E., Pedersen J. O. P., Polny J., Reichl U., Seinfeld J. H., Sipilä M., Stozhkov Y., Stratmann F., Svensmark H., Svensmark J., Veenhof R., Verheggen B., Viisanen Y., Wagner P. E., Wehrle G., Weingartner E., Wex H., Wilhelmsson M., Winkler P. M.: Results from the CERN pilot CLOUD experiment, 1680-7316, 1635-1647 pp. (2010).

Ehn M., Junninen H., Petäjä T., Kurtén T., Kerminen V. M., Schobesberger S., Manninen H. E., Ortega I. K., Vehkamäki H., Kulmala M., Worsnop D. R.: Composition and temporal behavior of ambient ions in the boreal forest, *Atmos. Chem. Phys.*, 10, 8513-8530 (2010).

Ehn M., Junninen H., Schobesberger S., Manninen H. E., Franchin A., Sipilä M., Petäjä T., Kerminen V.-M., Tammet H., Mirme A., Mirme S., Hõrrak U., Kulmala M., Worsnop D. R.: An instrumental comparison of mobility and mass measurements of atmospheric small ions, *Aerosol Sci. Tech.*, 45, 522-532 (2011).

Ehn M., Kleist E., Junninen H., Petäjä T., Lönn G., Schobesberger S., Dal Maso M., Trimborn A., Kulmala M., Worsnop D. R., Wahner A., Wildt J., Mentel T. F.: Gas phase formation of extremely oxidized pinene reaction products in chamber and ambient air, *Atmos. Chem. Phys.*, 12, 5113–5127 (2012).

Eisele F. L., Tanner D. J.: Measurement of the gas phase concentration of H_2SO_4 and methane sulfonic acid and estimates of H_2SO_4 production and loss in the atmosphere, *J. Geophys. Res.*, 98, 9001-9010 (1993).

Flagan R. C.: History of electrical aerosol measurements, *Aerosol Sci. Tech.*, 28, 301-380 (1998).

Fletcher N. H.: Size effect in heterogeneous nucleation, *J. Chem. Phys*, 29, 572-576 (1958).

Fletcher N. H.: *The Physics of Rainclouds*, Cambridge University Press (1962).

Froyd K. D., Lovejoy E. R.: Bond energies and structures of ammonia-sulfuric acid positive cluster ions, *J. Phys. Chem. A*, 116, 5886-5899 (2012).

Fuchs N. A.: On the stationary charge distribution on aerosol particles in a bipolar ionic atmosphere, *Geofisica Pura e Applicata*, 56, 185-193 (1963).

Gaman A. I., Napari I., Winkler P. M., Wagner P. E., Strey R., Viisanen Y., Kulmala M.: Homogeneous nucleation of n-nonane and n-propanol mixtures: A comparison of classical nucleation theory and experiments, *J. Chem. Phys.*, 123, 244502 (2005).

Gao J., Wang T., Zhou X., Wu W., Wang W.: Measurement of aerosol number size distributions in the Yangtze River delta in China: Formation and growth of particles under polluted conditions, *Atmos. Env.*, 43, 829-836 (2009).

Ge X., Wexler A. S., Clegg S. L.: Atmospheric amines – Part I. A review, *Atmos. Env.*, 45, 524-546 (2011).

Girshick S. L., Chiu C.-P.: Kinetic nucleation theory: A new expression for the rate of homogeneous nucleation from an ideal supersaturated vapor, *J. Chem. Phys.*, 93, 1273-1277 (1990).

Hallar A. G., Lowenthal D. H., Chirokova G., Borys R. D., Wiedinmyer C.: Persistent daily new particle formation at a mountain-top location, *Atmos. Env.*, 45, 4111-4115 (2011).

Hallquist M., Wenger J. C., Baltensperger U., Rudich Y., Simpson D., Claeys M., Dommen J., Donahue N. M., George C., Goldstein A. H., Hamilton J. F., Herrmann H., Hoffmann T., Iinuma Y., Jang M., Jenkin M. E., Jimenez J. L., Kiendler-Scharr A., Maenhaut W., McFiggans G., Mentel T. F., Monod A., Prevot A. S. H., Seinfeld J. H., Surratt J. D., Szmigielski R., Wildt J.: The formation, properties and impact of secondary organic aerosol: current and emerging issues, *Atmos. Chem. Phys.*, 9, 5155-5236 (2009).

Hamburger T., McMeeking G., Minikin A., Birmili W., Dall'Osto M., O'Dowd C. D., Flentje H., Henzing B., Junninen H., Kristensson A., de Leeuw G., Stohl A., Burkhart J. F., Coe H., Krejci R., Petzold A.: Overview of the synoptic and pollution situation

over Europe during the EUCAARI-LONGREX field campaign, *Atmos. Chem. Phys.*, 11, 1065-1082 (2011).

Hanson D. R., Eisele F. L.: Measurement of prenucleation molecular clusters in the NH_3, H_2SO_4, H_2O system, *J. Geophys. Res.*, 107, AAC 10-11-AAC 10-18 (2002).

Hanson D. R., McMurry P. H., Jiang J., Tanner D., Huey L. G.: Ambient pressure proton transfer mass spectrometry: Detection of amines and ammonia, *Environ. Sci. Technol.*, 45, 8881-8888 (2011).

Hari P., Kulmala M.: Station for Measuring Ecosystem-Atmosphere Relations (SMEAR II), *Boreal Env. Res.*, 10, 315-322 (2005).

Hari P., Andreae M. O., Kabat P., Kulmala M.: A comprehensive network of measuring stations to monitor climate change, *Boreal Env. Res.*, 14, 442-446 (2009).

Hegg D. A., Radke L. F., Hobbs P. V.: Particle production associated with marine clouds, *J. Geophys. Res.*, 95, 13917-13926 (1990).

Hienola A. I., Winkler P. M., Wagner P. E., Vehkamäki H., Lauri A., Napari I., Kulmala M.: Estimation of line tension and contact angle from heterogeneous nucleation experimental data, *J. Chem. Phys.*, 126, 094705 (2007).

Hinds W. C.: *Aerosol Technology: Properties, Behavior, and Measurement of Airborne Particles - 2nd ed.*, John Wiley & Sons (1999).

Hussein T., Junninen H., Tunved P., Kristensson A., Dal Maso M., Riipinen I., Aalto P. P., Hansson H.-C., Swietlicki E., Kulmala M.: Time span and spatial scale of regional new particle formation events over Finland and Southern Sweden, *Atmos. Chem. Phys.*, 9, 4699-4716 (2009).

Iida K., Stolzenburg M. R., McMurry P. H.: Effect of working fluid on sub-2 nm particle detection with a laminar flow ultrafine condensation particle counter, *Aerosol Sci. Tech.*, 43, 81-96 (2009).

IPCC: Climate Change 2007: The Physical Science Basis. Contribution of Working Group I to the Fourth Assessment Report of the Intergovernmental Panel on Climate Change [Solomon S., Qin D., M. M., Chen Z., Marquis M., Averyt K. B., Tignor M., Miller H. L. (Eds.)], Cambridge University Press, Cambridge, UK, and New York, NY, USA (2007).

Jaenicke R.: Tropospheric aerosols. In: *Aerosol-Cloud-Climate Interactions*, [Hobbs P. V. (Ed.)], Academic Press, San Diego, CA, USA (1993).

Järvinen E., Virkkula A., Nieminen T., Aalto P. P., Asmi E., Lanconelli C., Busetto M., Lupi A., Schioppo R., Vitale V., Mazzola M., Petäjä T., Kerminen V. M., Kulmala M.: Seasonal cycle and modal structure of particle number size distribution at Dome C, Antarctica, *Atmos. Chem. Phys.*, 13, 7473-7487 (2013).

Jennings K. R.: Collision-induced decompositions of aromatic molecular ions, *Int. J. Mass Spectrom. Ion Phys.*, 1, 227-235 (1968).

Jimenez J. L., Canagaratna M. R., Donahue N. M., Prevot A. S. H., Zhang Q., Kroll J. H., DeCarlo P. F., Allan J. D., Coe H., Ng N. L., Aiken A. C., Docherty K. S., Ulbrich I. M., Grieshop A. P., Robinson A. L., Duplissy J., Smith J. D., Wilson K. R., Lanz V. A., Hueglin C., Sun Y. L., Tian J., Laaksonen A., Raatikainen T., Rautiainen J., Vaattovaara P., Ehn M., Kulmala M., Tomlinson J. M., Collins D. R., Cubison M. J., Dunlea E. J., Huffman J. A., Onasch T. B., Alfarra M. R., Williams P. I., Bower K., Kondo Y., Schneider J., Drewnick F., Borrmann S., Weimer S., Demerjian K., Salcedo D., Cottrell L., Griffin R., Takami A., Miyoshi T., Hatakeyama S., Shimono A., Sun J. Y., Zhang Y. M., Dzepina K., Kimmel J. R., Sueper D., Jayne J. T., Herndon S. C., Trimborn A. M., Williams L. R., Wood E. C., Middlebrook A. M., Kolb C. E., Baltensperger U., Worsnop D. R.: Evolution of organic aerosols in the atmosphere, *Science*, 326, 1525-1529 (2009).

Jung J., Miyazaki Y., Kawamura K.: Different characteristics of new particle formation between urban and deciduous forest sites in Northern Japan during the summers of 2010–2011, *Atmos. Chem. Phys.*, 13, 51-68 (2013).

Junninen H., Ehn M., Petäjä T., Luosujärvi L., Kotiaho T., Kostiainen R., Rohner U., Gonin M., Fuhrer K., Kulmala M., Worsnop D. R.: A high-resolution mass spectrometer to measure atmospheric ion composition, *Atmos. Meas. Tech.*, 3, 1039-1053 (2010).

Kerminen V.-M., Petäjä T., Manninen H. E., Paasonen P., Nieminen T., Sipilä M., Junninen H., Ehn M., Gagné S., Laakso L., Riipinen I., Vehkamäki H., Kurtén T., Ortega I. K., Dal Maso M., Brus D., Hyvärinen A., Lihavainen H., Leppä J., Lehtinen K. E. J., Mirme A., Mirme S., Hõrrak U., Berndt T., Stratmann F., Birmili W., Wiedensohler A., Metzger A., Dommen J., Baltensperger U., Kiendler-Scharr A., Mentel T. F., Wildt J., Winkler P. M., Wagner P. E., Petzold A., Minikin A., Plass-Dülmer C., Pöschl U., Laaksonen A., Kulmala M.: Atmospheric nucleation: Highlights of the EUCAARI project and future directions, *Atmos. Chem. Phys.*, 10, 10829-10848 (2010).

Kirkby J., Curtius J., Almeida J., Dunne E., Duplissy J., Ehrhart S., Franchin A., Gagné S., Ickes L., Kürten A., Kupc A., Metzger A., Riccobono F., Rondo L., Schobesberger S., Tsagkogeorgas G., Wimmer D., Amorim A., Bianchi F., Breitenlechner M., David A., Dommen J., Downard A., Ehn M., Flagan R. C., Haider S., Hansel A., Hauser D., Jud W., Junninen H., Kreissl F., Kvashin A., Laaksonen A., Lehtipalo K., Lima J., Lovejoy E. R., Makhmutov V., Mathot S., Mikkilä J., Minginette P., Mogo S., Nieminen T., Onnela A., Pereira P., Petäjä T., Schnitzhofer R., Seinfeld J. H., Sipilä M., Stozhkov Y., Stratmann F., Tomé A., Vanhanen J., Viisanen Y., Vrtala A., Wagner P. E., Walther H., Weingartner E., Wex H., Winkler P. M., Carslaw K. S., Worsnop D. R., Baltensperger U., Kulmala M.: Role of sulphuric acid, ammonia and galactic cosmic rays in atmospheric aerosol nucleation, *Nature*, 476, 429-433 (2011).

Köhler H.: The nucleus in and the growth of hygroscopic droplets, *Trans. Farad. Soc.*, 32, 1152-1161 (1936).

Komppula M., Sihto S. L., Korhonen H., Lihavainen H., Kerminen V. M., Kulmala M., Viisanen Y.: New particle formation in air mass transported between two measurement sites in Northern Finland, *Atmos. Chem. Phys.*, 6, 2811-2824 (2006).

Krämer L., Pöschl U., Niessner R.: Microstructural rearrangement of sodium chloride condensation aerosol particles on interaction with water vapor, *J. Aerosol Sci.*, 31, 673-685 (2000).

Kroll J. H., Donahue N. M., Jimenez J. L., Kessler S. H., Canagaratna M. R., Wilson K. R., Altieri K. E., R.Mazzoleni L., Wozniak A. S., Bluhm H., Mysak E. R., Smith J. D., Kolb C. E., Worsnop D. R.: Carbon oxidation state as a metric for describing the chemistry of atmospheric organic aerosol, *Nature Chem.*, 3, 133-139 (2011).

Kuang C., McMurry P. H., McCormick A. V., Eisele F. L.: Dependence of nucleation rates on sulfuric acid vapor concentration in diverse atmospheric locations, *J. Geophys. Res.*, 113, D10209 (2008).

Kuang C., Chen M., Zhao J., Smith J., McMurry P. H., Wang J.: Size and time-resolved growth rate measurements of 1 to 5nm freshly formed atmospheric nuclei, *Atmos. Chem. Phys.*, 12, 3573-3589 (2012).

Kulmala M., Viisanen Y.: Homogeneous nucleation: Reduction of binary nucleation to homomolecular nucleation, *J. Aerosol Sci.*, 22, S97-S100 (1991).

Kulmala M., Rannik Ü., Zapadinsky E. L., Clement C. F.: The effect of saturation fluctuations on droplet growth, *J. Aerosol Sci.*, 28, 1395-1409 (1997).

Kulmala M., Pirjola L., Mäkelä J. M.: Stable sulphate clusters as a source of new atmospheric particles, *Nature*, 404, 66-69 (2000).

Kulmala M., Dal Maso M., Mäkelä J. M., Pirjola L., Väkevä M., Aalto P., Miikkulainen P., Hämeri K., O'Dowd C.: On the formation, growth and composition of nucleation mode particles, *Tellus B*, 53, 479-490 (2001a).

Kulmala M., Hämeri K., Aalto P. P., Mäkelä J. M., Pirjola L., Douglas Nilsson E., Buzorius G., Rannik Ü., Dal Maso M., Seidl W., Hoffman T., Janson R., Hansson H.-C., Viisanen Y., Laaksonen A., O'Dowd C. D.: Overview of the international project on biogenic aerosol formation in the boreal forest (BIOFOR), *Tellus*, 53B, 324-343 (2001b).

Kulmala M., Kerminen V.-M., Anttila T., Laaksonen A., O'Dowd C. D.: Organic aerosol formation via sulphate cluster activation, *J. Geophys. Res.*, 109, D04205 (2004a).

Kulmala M., Suni T., Lehtinen K. E. J., Dal Maso M., Boy M., Reissell A., Rannik U., Aalto P., Keronen P., Hakola H., Bäck J., Hoffmann T., Vesala T., Hari P.: A new

feedback mechanism linking forests, aerosols, and climate, *Atmos. Chem. Phys.*, 4, 557-562 (2004b).

Kulmala M., Vehkamäki H., Petäjä T., Dal Maso M., Lauri A., Kerminen V.-M., Birmili W., McMurry P. H.: Formation and growth rates of ultrafine atmospheric particles: a review of observations, *J. Aerosol Sci.*, 35, 143-176 (2004c).

Kulmala M., Mordas G., Petäjä T., Grönholm T., Aalto P. P., Vehkamäki H., Hienola A. I., Herrmann E., Sipilä M., Riipinen I., Manninen H. E., Hämeri K., Stratmann F., Bilde M., Winkler P. M., Birmili W., Wagner P. E.: The condensation particle counter battery (CPCB): A new tool to investigate the activation properties of nanoparticles, *J. Aerosol Sci.*, 38, 289-304 (2007).

Kulmala M., Kerminen V.-M.: On the formation and growth of atmospheric nanoparticles, *Atmos. Res.*, 90, 132-150 (2008).

Kulmala M., Petäjä T., Nieminen T., Sipilä M., Manninen H. E., Lehtipalo K., Dal Maso M., Aalto P. P., Junninen H., Paasonen P., Riipinen I., Lehtinen K. E. J., Laaksonen A., Kerminen V.-M.: Measurement of the nucleation of atmospheric aerosol particles, *Nat. Protoc.*, 7, 1651-1667 (2012).

Kulmala M., Kontkanen J., Junninen H., Lehtipalo K., Manninen H. E., Nieminen T., Petäjä T., Sipilä M., Schobesberger S., Rantala P., Franchin A., Jokinen T., Järvinen E., Äijälä M., Kangasluoma J., Hakala J., Aalto P. P., Paasonen P., Mikkilä J., Vanhanen J., Aalto J., Hakola H., Makkonen U., Ruuskanen T., Mauldin R. L., 3rd, Duplissy J., Vehkamäki H., Bäck J., Kortelainen A., Riipinen I., Kurtén T., Johnston M. V., Smith J. N., Ehn M., Mentel T. F., Lehtinen K. E., Laaksonen A., Kerminen V.-M., Worsnop D. R.: Direct observations of atmospheric aerosol nucleation, *Science*, 339, 943-946 (2013).

Kupc A., Amorim A., Curtius J., Danielczok A., Duplissy J., Ehrhart S., Walther H., Ickes L., Kirkby J., Kürten A., Lima J. M., Mathot S., Minginette P., Onnela A., Rondo L., Wagner P. E.: A fibre-optic UV system for H_2SO_4 production in aerosol chambers causing minimal thermal effects, *J. Aerosol Sci.*, 42, 532–543 (2011).

Kürten A., Rondo L., Ehrhart S., Curtius J.: Performance of a corona ion source for measurement of sulfuric acid by chemical ionization mass spectrometry, *Atmos. Meas. Tech.*, 4, 437-443 (2011).

Kürten A., Rondo L., Ehrhart S., Curtius J.: Calibration of a chemical ionization mass spectrometer for the measurement of gaseous sulfuric acid, *J. Phys. Chem. A*, 116, 6375-6386 (2012).

Kurtén T., Torpo L., Ding C.-G., Vehkamäki H., Sundberg M. R., Laasonen K., Kulmala M.: A density functional study on water-sulfuric acid-ammonia clusters and implications for atmospheric cluster formation, *J. Geophys. Res.*, 112, D04210 (2007).

Kurtén T., Loukonen V., Vehkamäki H., Kulmala M.: Amines are likely to enhance neutral and ion-induced sulfuric acid-water nucleation in the atmosphere more effectively than ammonia, *Atmos. Chem. Phys.*, 8, 4095-4103 (2008).

Kurtén T., Petäjä T., Smith J., Ortega I. K., Sipilä M., Junninen H., Ehn M., Vehkamäki H., Mauldin L., Worsnop D. R., Kulmala M.: The effect of H_2SO_4 – amine clustering on chemical ionization mass spectrometry (CIMS) measurements of gas-phase sulfuric acid, *Atmos. Chem. Phys.*, 11, 3007-3019 (2011).

Laaksonen A., Korhonen P., Kulmala M., Charlson R. J.: Modification of the Köhler equation to include soluble trace gases and slightly soluble substance, *J. Atmos. Sci.*, 55, 853-862 (1998).

Lee S.-H., Reeves J. M., Wilson J. C., Hunton D. E., Viggiano A. A., Miller T. M., Ballenthin J. O., Lait L. R.: Particle formation by ion nucleation in the upper troposphere and lower stratosphere, *Science*, 301, 1886-1889 (2003).

Lovejoy E. R., Curtius J., Froyd K. D.: Atmospheric ion-induced nucleation of sulfuric acid and water, *J. Geophys. Res.*, 109, D08204 (2004).

Mäkelä J. M., Aalto P. P., Jokinen V., Pohja T., Nissinen A., Palmroth S., Markkanen T., Seitsonen K., Lihavainen H., Kulmala M.: Observations of ultrafine aerosol particle formation and growth in boreal forest, *Geophys. Res. Lett.*, 24, 1219-1222 (1997).

Mäkelä J. M., Yli-Koivisto S., Hiltunen V., Seidl W., Swietlicki E., Teinilä K., Sillanpää M., Koponen I. K., Paatero J., Rosman K., Hämeri K.: Chemical composition of aerosol during particle formation events in boreal forest, *Tellus*, 53B, 380-393 (2001).

Manninen H. E., Petäjä T., Asmi E., Riipinen I., Nieminen T., Mikkilä J., Hõrrak U., Mirme A., Mirme S., Laakso L., Kerminen V.-M., Kulmala M.: Long-term field measurements of charged and neutral clusters using neutral cluster and air ion spectrometer (NAIS), *Boreal Env. Res.*, 14, 591-605 (2009).

Manninen H. E., Nieminen T., Asmi E., Gagné S., Häkkinen S., Lehtipalo K., Aalto P. P., Vana M., Mirme A., Mirme S., Hõrrak U., Plass-Dülmer C., Stange G., Kiss G., Hoffer A., Törö N., Moerman M., Henzing B., de Leeuw G., Brinkenberg M., Kouvarakis G. N., Bougiatioti A., Mihalopoulos N., O'Dowd C., Ceburnis D., Arneth A., Svenningsson B., Swietlicki E., Tarozzi L., Decesari S., Facchini M. C., Birmili W., Sonntag A., Wiedensohler A., Boulon J., Sellegri K., Laj P., Gysel M., Bukowiecki N., Weingartner E., Wehrle G., Laaksonen A., Hamed A., Joutsensaari J., Petäjä T., Kerminen V.-M., Kulmala M.: EUCAARI ion spectrometer measurements at 12 European sites – analysis of new particle formation events, *Atmos. Chem. Phys.*, 10, 7907–7927 (2010).

Marti J. J., Jefferson A., Cai X. P., Richert C., McMurry P. H., Eisele F.: H2SO4 vapor pressure of sulfuric acid and ammonium sulfate solutions, *J. Geophys. Res.*, 102, 3725-3735 (1997).

McGrath M. J., Olenius T., Ortega I. K., Loukonen V., Paasonen P., Kurtén T., Kulmala M., Vehkamäki H.: Atmospheric cluster dynamics code: a flexible method for solution of the birth-death equations, *Atmos. Chem. Phys.*, 12, 2345-2355 (2012).

McGraw R., Wang J., Kuang C.: Kinetics of heterogeneous nucleation in supersaturated vapor: Fundamental limits to neutral particle detection revisited, *Aerosol Sci. Tech.*, 46, 1053-1064 (2012).

McMurry P. H.: A review of atmospheric aerosol measurements, *Atmos. Env.*, 34, 1959-1999 (2000).

McNaughton C. S., Clarke A. D., Howell S. G., Pinkerton M., Anderson B., Thornhill L., Hudgins C., Winstead E., Dibb J. E., Scheuer E., Maring H.: Results from the DC-8 inlet characterization experiment (DICE): Airborne versus surface sampling of mineral dust and sea salt aerosols, *Aerosol Sci. Tech.*, 41, 136-159 (2007).

Merikanto J., Spracklen D. V., Mann G. W., Pickering S. J., Carslaw K. S.: Impact of nucleation on global CCN, *Atmos. Chem. Phys.*, 9, 8601-8616 (2009).

Metzger A., Verheggen B., Dommen J., Duplissy J., Prevot A. S. H., Weingartner E., Riipinen I., Kulmala M., Spracklen D. V., Carslaw K. S., Baltensperger U.: Evidence for the role of organics in aerosol particle formation under atmospheric conditions, *Proc. Natl. Acad. Sci. USA*, 107, 6646-6651 (2010).

Mikhailov E., Vlasenko S., Martin S. T., Koop T., Pöschl U.: Amorphous and crystalline aerosol particles interacting with water vapor: conceptual framework and experimental evidence for restructuring, phase transitions and kinetic limitations, *Atmos. Chem. Phys.*, 9, 9491-9522 (2009).

Mirme S., Mirme A., Minikin A., Petzold A., Hõrrak U., Kerminen V.-M., Kulmala M.: Atmospheric sub-3nm particles at high altitudes, *Atmos. Chem .Phys.*, 10, 437-451 (2010).

Mönkkönen P., Koponen I. K., Lehtinen K. E. J., Hämeri K., Uma R., Kulmala M.: Measurements in a highly polluted Asian mega city: observations of aerosol number size distribution, modal parameters and nucleation events, *Atmos. Chem. Phys.*, 5, 57-66 (2005).

Nel A., Xia T., Mädler L., Li N.: Toxic potential of materials at the nanolevel, *Science*, 311, 622-627 (2006).

Nilsson E. D., Rannik Ü., Kulmala M., Buzorius G., O´Dowd C. D.: Effects of the continental boundary layer evolution, convection, turbulence and entrainment on aerosol tormation, *Tellus*, 53B, 441-461 (2001).

Norman M., Hansel A., Wisthaler A.: O_2^+ as reagent ion in the PTR-MS instrument: Detection of gas-phase ammonia, *Int. J. Mass. Spectrom.*, 265, 382-387 (2007).

O'Dowd C. D., Hämeri K., Mäkelä J., Väkeva M., Aalto P., de Leeuw G., Kunz G. J., Becker E., Hansson H.-C., Allen A. G., Harrison R. M., Berresheim H., Kleefeld C., Geever M., Jennings S. G., Kulmala M.: Coastal new particle formation: Environmental conditions and aerosol physicochemical characteristics during nucleation bursts, *J. Geophys. Res.*, 107, 8107 (2002).

O'Dowd C. D., Yoon Y. J., Junkermann W., Aalto P. P., Kulmala M., Lihavainen H., Viisanen Y.: Airborne measurements of nucleation mode particles I: coastal nucleation and growth rates, *Atmos. Chem. Phys.*, 7, 1491-1501 (2007).

O'Dowd C. D., Yoon Y. J., Junkermann W., Aalto P. P., Kulmala M., Lihavainen H., Viisanen Y.: Airborne measurements of nucleation mode particles II: boreal forest nucleation events, *Atmos. Chem. Phys.*, 9, 937-944 (2009).

Ortega I. K., Kurtén T., Vehkamäki H., Kulmala M.: The role of ammonia in sulfuric acid ion induced nucleation, *Atmos. Chem. Phys.*, 8, 2859-2867 (2008).

Ortega I. K., Kupiainen O., Kurtén T., Olenius T., Wilkman O., McGrath M. J., Loukonen V., Vehkamäki H.: From quantum chemical formation free energies to evaporation rates, *Atmos. Chem. Phys.*, 12, 225–235 (2012).

Paasonen P., Nieminen T., Asmi E., Manninen H. E., Petaja T., Plass-Dulmer C., Flentje H., Birmili W., Wiedensohler A., Horrak U., Metzger A., Hamed A., Laaksonen A., Facchini M. C., Kerminen V.-M., Kulmala M.: On the roles of sulphuric acid and low-volatility organic vapours in the initial steps of atmospheric new particle formation, *Atmos. Chem. Phys.*, 10, 11223-11242 (2010).

Paasonen P., Olenius T., Kupiainen O., Kurtén T., Petäjä T., Birmili W., Hamed A., Hu M., Huey L. G., Plass-Duelmer C., Smith J. N., Wiedensohler A., Loukonen V., McGrath M. J., Ortega I. K., Laaksonen A., Vehkamäki H., Kerminen V.-M., Kulmala M.: On the formation of sulphuric acid – amine clusters in varying atmospheric conditions and its influence on atmospheric new particle formation, *Atmos. Chem. Phys.*, 12, 9113-9133 (2012).

Petäjä T., Sipilä M., Paasonen P., Nieminen T., Kurtén T., Ortega I. K., Stratmann F., Vehkamäki H., Berndt T., Kulmala M.: Experimental observation of strongly bound dimers of sulfuric acid: Application to nucleation in the atmosphere, *Phys. Rev. Lett.*, 106, 228302 (2011).

Petersen D., Ortner R., Vrtala A., Wagner P. E., Kulmala M., Laaksonen A.: Soluble-insoluble transition in binary heterogeneous nucleation, *Phys. Rev. Lett.*, 87, 225703 (2001).

Praplan A. P., Bianchi F., Dommen J., Baltensperger U.: Dimethylamine and ammonia measurements with ion chromatography during the CLOUD4 campaign, *Atmos. Meas. Tech.*, 5, 2161-2167 (2012).

Pryor S. C., Barthelmie R. J., Sørensen L. L., McGrath J. G., Hopke P., Petäjä T.: Spatial and vertical extent of nucleation events in the Midwestern USA: Insights from the Nucleation In ForesTs (NIFTy) experiment, *Atmos. Chem. Phys.*, 11, 1641-1657 (2011).

Raes F., Janssens A.: Ion-induced aerosol formation in a H_2O-H_2SO_4 system - I. Extension of the classical theory and search for experimental evidence, *J. Aerosol Sci.*, 16, 217-227 (1985).

Raoult F.-M.: Loi générale des tensions de vapeur des dissolvants, *Comptes rendus*, 104, 1430-1433 (1887).

Raoult F.-M.: Über die Dampfdrucke ätherische Lösungen, *Z. Phys. Chem.*, 2, 353-373 (1888).

Reischl G. P.: Measurement of ambient aerosols by the differential mobility analyzer method - concepts and realization citeria for the size range between 2-nm and 500-nm, *Aerosol Sci. Tech.*, 14, 5-24 (1991).

Reischl G. P., Makela J. M., Necid J.: Performance of Vienna type differential mobility analyzer at 1.2-20 nanometer, *Aerosol Sci. Tech.*, 27, 651-672 (1997).

Riccobono F., Rondo L., Sipilä M., Barmet P., Curtius J., Dommen J., Ehn M., Ehrhart S., Kulmala M., Kürten A., Mikkilä J., Paasonen P., Petäjä T., Weingartner E., Baltensperger U.: Contribution of sulfuric acid and oxidized organic compounds to particle formation and growth, *Atmos. Chem. Phys.*, 12, 9427-9439 (2012).

Riipinen I., Sihto S.-L., Kulmala M., Arnold F., Dal Maso M., Birmili W., Saarnio K., Teinilä K., Kerminen V.-M., Laaksonen A., Lehtinen K. E. J.: Connections between atmospheric sulphuric acid and new particle formation during QUEST III-IV campaigns in Heidelberg and Hyytiälä, *Atmos. Chem. Phys.*, 7, 1899-1914 (2007).

Riipinen I., Manninen H. E., Yli-Juuti T., Boy M., Sipilä M., Ehn M., Junninen H., Petäjä T., Kulmala M.: Applying the condensation particle counter battery (CPCB) to study the water-affinity of freshly-formed 2-9 nm particles in boreal forest, *Atmos. Chem. Phys.*, 9, 3317-3330 (2009).

Riipinen I., Yli-Juuti T., Pierce J. R., Petaja T., Worsnop D. R., Kulmala M., Donahue N. M.: The contribution of organics to atmospheric nanoparticle growth, *Nat. Geosci.*, 5, 453-458 (2012).

Scheibel H. G., Porstendörfer J.: Generation of monodisperse Ag- and NaCl-aerosols with particle diameters between 2 and 300nm, *J. Aerosol Sci.*, 14, 113-126 (1983).

Scorer R. S.: Ship trails, *Atmos. Env.*, 21, 1417-1425 (1967).

Seinfeld J. H., Pandis S. N.: *Atmospheric Chemistry and Physics: From Air Pollution to Climate Change - 2nd ed.*, John Wiley & Sons, Hoboken, NJ, USA (2006).

Shen X. J., Sun J. Y., Zhang Y. M., Wehner B., Nowak A., Tuch T., Zhang X. C., Wang T. T., Zhou H. G., Zhang X. L., Dong F., Birmili W., Wiedensohler A.: First long-term study of particle number size distributions and new particle formation events of regional aerosol in the North China Plain, *Atmos. Chem. Phys.*, 11, 1565-1580 (2011).

Sihto S.-L., Kulmala M., Kerminen V.-M., Dal Maso M., Petäjä T., Riipinen I., Korhonen H., Arnold F., Janson R., Boy M., Laaksonen A., Lehtinen K. E. J.: Atmospheric sulphuric acid and aerosol formation: Implications from atmospheric measurements for nucleation and early growth mechanisms, *Atmos. Chem. Phys.*, 6, 4079-4091 (2006).

Singh H. B., Anderson B. E., Avery M. A., Viezee W., Chen Y., Tabazadeh A., Hamill P., Pueschel R., Fuelberg H. E., Hannan J. R.: Global distribution and sources of volatile and nonvolatile aerosol in the remote troposphere, *J. Geophys. Res.*, 107, ACH 7-1-ACH 7-10 (2002).

Sipilä M., Berndt T., Petäjä T., Brus D., Vanhanen J., Stratmann F., Patokoski J., Mauldin R. L., Hyvärinen A. P., Lihavainen H., Kulmala M.: The role of sulfuric acid in atmospheric nucleation, *Science*, 327, 1243-1246 (2010).

Smith J. N., Barsanti K. C., Friedli H. R., Ehn M., Kulmala M., Collins D. R., Scheckman J. H., Williams B. J., McMurry P. H.: Observations of aminium salts in atmospheric nanoparticles and possible climatic implications, *Proc. Natl. Acad. Sci. USA*, 107, 6634-6639 (2010).

Strey R., Viisanen Y., Wagner P. E.: Measurements of the molar content of binary nuclei. III. Use of the nucleation rate surfaces for the water-n-alcohol series, *J. Chem. Phys.*, 103, 4333 (1995).

Thomson J. J.: *Conduction of Electricity through Gases*, Cambridge University Press, London (1906).

Thomson W.: On the equilibrium of vapour at a curved surface of liquid, *Proc. Roy. Soc. Edinburgh*, 7, 63-69 (1870).

Thomson W.: On the equilibrium of vapour at a curved surface of liquid, *Phil. Mag.*, 42, 448-452 (1871).

Twohy C. H., Clement C. F., Gandrud B. W., Weinheimer A. J., Campos T. L., Baumgardner D., Brune W. H., Sachse G. W., Vay S. A.: Deep convection as a source of new particles in the midlatitude upper troposphere, *J. Geophys. Res.*, 107, AAC 6-1–AAC 6-10 (2002).

Vaclavik Bräuner E., Forchhammer L., Møller P., Simonsen J., Glasius M., Wåhlin P., Raaschou-Nielsen O., Loft S.: Exposure to ultrafine particles from ambient air and oxidative stress-induced DNA damage, *Environ. Health Perspect.*, 115, 1177-1182 (2007).

Vanhanen J., Mikkilä J., Lehtipalo K., Sipilä M., Manninen H. E., Siivola E., Petäjä T., Kulmala M.: Particle size magnifier for nano-CN detection, *Aerosol Sci. Tech.*, 45, 533-542 (2011).

Vehkamäki H., Kulmala M., Napari I., Lehtinen K. E. J., Timmreck C., Noppel M., Laaksonen A.: An improved parameterization for sulfuric acid/water nucleation rates for tropospheric and stratospheric conditions, *J. Geophys. Res.*, 107, AAC 3-1–AAC 3-10 (2002).

Vehkamäki H.: *Classical Nucleation Theory in Multicomponent Systems,* Springer-Verlag, Berlin Heidelberg (2006).

Vehkamäki H., Määttänen A., Lauri A., Kulmala M., Winkler P., Vrtala A., Wagner P. E.: Heterogeneous multicomponent nucleation theorems for the analysis of nanoclusters, *J. Chem. Phys.*, 126, 174707 (2007).

Vehkamäki H., Riipinen I.: Thermodynamics and kinetics of atmospheric aerosol particle formation and growth, *Chem. Soc. Rev.*, 41, 5160-5173 (2012).

Venzac H., Sellegri K., Laj P., Villani P., Bonasoni P., Marinoni A., Cristofanelli P., Calzolari F., Fuzzi S., Decesari S., Facchini M. C., Vuillermoz E., Verza G. P.: High frequency new particle formation in the Himalayas, *Proc. Natl. Acad. Sci. USA*, 105, 15666-15671 (2008).

Viisanen Y., Strey R., Laaksonen A., Kulmala M.: Measurements of the molecular content of binary nuclei. II. Use of the nucleation rate surface for water-ethanol, *J. Chem. Phys.*, 100, 6062-6072 (1994).

Voigtländer J., Duplissy J., Rondo L., Kürten A., Stratmann F.: Numerical simulations of mixing conditions and aerosol dynamics in the CERN CLOUD chamber, *Atmos. Chem. Phys.*, 12, 2205-2214 (2012).

Wagner P. E.: A constant-angle mie scattering method (CAMS) for investigation of particle formation processes, *J. Colloid Interface Sci.*, 105, 456 (1985).

Wagner P. E., Kaller D., Vrtala A., Lauri A., Kulmala M., Laaksonen A.: Nucleation probability in binary heterogeneous nucleation of water-n-propanol vapor mixtures on insoluble and soluble nanoparticles, *Phys. Rev. E*, 67, 021605 (2003).

Wang L., Khalizov A. F., Zheng J., Xu W., Ma Y., Lal V., Zhang R.: Atmospheric nanoparticles formed from heterogeneous reactions of organics, *Nat. Geosci.*, 3, 238-242 (2010).

Wang S. C., Flagan R. C.: Scanning electrical mobility spectrometer, *Aerosol Sci. Tech.*, 13, 230-240 (1990).

Weber R. J., Marti J., McMurry P. H., Eisele F. L., Tanner D. J., Jefferson A.: Measured atmospheric new particle formation rates: implications for nucleation mechanisms, *Chem. Eng. Comm*, 151, 53-64 (1996).

Weber R. J., McMurry P. H., Mauldin R. L., Tanner D., Eisele F. L., Clarke A. D., Kapustin V.: New particle formation in the remote troposphere: A comparison of observations at various sites, *Geophys. Res. Lett.*, 26, 307-310 (1999).

Weber R. J., Chen G., Davis D. D., Mauldin III R. L., Tanner D. J., Eisele F. L., Clarke A. D., Thornton D. C., Bandy A. R.: Measurements of enhanced H_2SO_4 and 3-4nm particles near a frontal cloud during the First Aerosol Characterization Experiment (ACE 1), *J. Geophys. Res.*, 106, 24107-24117 (2001).

Wehner B., Siebert H., Stratmann F., Tuch T., Wiedensohler A., Petäjä T., Dal Maso M., Kulmala M.: Horizontal homogeneity and vertical extent of new particle formation events, *Tellus*, 59B, 362-371 (2007).

Wehner B., Siebert H., Ansmann A., Ditas F., Seifert P., Stratmann F., Wiedensohler A., Apituley A., Shaw R. A., Manninen H. E., Kulmala M.: Observations of turbulence-induced new particle formation in the residual layer, *Atmos. Chem. Phys.*, 10, 4319-4330 (2010).

Weigel R., Borrmann S., Kazil J., Minikin A., Stohl A., Wilson J. C., Reeves J. M., Kunkel D., de Reus M., Frey W., Lovejoy E. R., Volk C. M., Viciani S., D'Amato F., Schiller C., Peter T., Schlager H., Cairo F., Law K. S., Shur G. N., Belyaev G. V., Curtius J.: In situ observations of new particle formation in the tropical upper troposphere: the role of clouds and the nucleation mechanism, *Atmos. Chem. Phys.*, 11, 9983-10010 (2011).

Wimmer D., Lehtipalo K., Franchin A., Kangasluoma J., Kreissl F., Kürten A., Kupc A., Metzger A., Mikkilä J., Petäjä T., Riccobono F., Vanhanen J., Kulmala M., Curtius J.: Performance of diethylene glycol-based particle counters in the sub-3 nm size range, *Atmos. Meas. Tech.*, 6, 1793-1804 (2013).

Winkler P. M., Steiner G., Vrtala A., Vehkamäki H., Noppel M., Lehtinen K. E. J., Reischl G. P., Wagner P. E., Kulmala M.: Heterogeneous nucleation experiments bridging the scale from molecular ion clusters to nanoparticles, *Science*, 319(5868), 1374-1377 (2008a).

Winkler P. M., Vrtala A., Wagner P. E.: Condensation particle counting below 2 nm seed particle diameter and the transition from heterogeneous to homogeneous nucleation, *Atmos. Res.*, 90, 125-131 (2008b).

Winkler P. M., Vrtala A., Steiner G., Wimmer D., Vehkamäki H., Lehtinen K. E. J., Reischl G. P., Kulmala M., Wagner P. E.: Quantitative characterization of critical

nanoclusters nucleated on large single molecules, *Phys. Rev. Lett.*, 108, 085701 (2012).

Wölk J., Strey R.: Homogeneous nucleation of H_2O and D_2O in comparison: The isotope effect, *J. Phys. Chem. B*, 105, 11683-11701 (2001).

Yu F.: Binary H_2SO_4-H_2O homogenous nucleation based on quasi-unary nucleation model: Look-up tables, *J. Geophys. Res.*, 111, D04201 (2006).

Yue G. K., Hamill P.: The homogeneous nucleation rates of H_2SO_4-H_2O aerosol particles in air, *J. Aerosol Sci.*, 10, 609-614 (1979).

Zhang R., Suh I., Zhao J., Zhang D., Fortner E. C., Tie X., Molina L. T., Molina M. J.: Atmospheric new particle formation enhanced by organic acids, *Science*, 304, 1487 (2004).

Zhang R., Wang L., Khalizov A. F., Zhao J., Zheng J., McGraw R. L., Molina L. T.: Formation of nanoparticles of blue haze enhanced by anthropogenic pollution, *Proc. Natl. Acad. Sci. USA*, 106, 17650-17654 (2009).

Zhao J., Khalizov A., Zhang R., McGraw R.: Hydrogen-bonding interaction in molecular complexes and clusters of aerosol nucleation precursors, *J. Phys. Chem. A*, 113, 680–689 (2009).